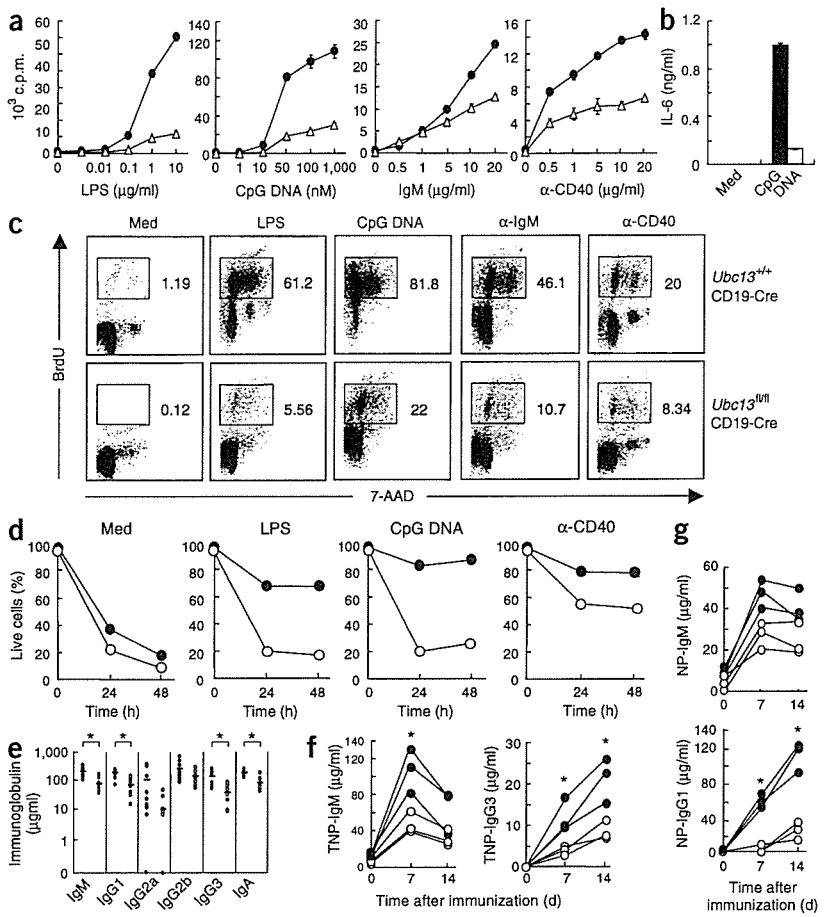

Figure 3 Ubc13 is required for B cell activation and *in vivo* immune responses. (**a**) Proliferation of splenic B220$^+$ B cells cultured for 48 h with various stimuli (horizontal axes). α-CD40, anti-CD40. Data are representative of three independent experiments. (**b**) ELISA of IL-6 in supernatants of splenic B220$^+$ B cells stimulated for 48 h with 1 μM CpG DNA. ND, not detected. Data represent mean ± s.d. of triplicate samples and are representative of two independent experiments. (**c**) Cell cycle profiles of B cells stimulated with 10 μg/ml of LPS, 1 μM CpG DNA, 10 μg/ml of anti-IgM or 10 μg/ml of anti-CD40. Cells labeled with 5-bromodeoxyuridine (BrdU) and 7-amino-actinomycin D (7-AAD) were analyzed by flow cytometry 24 h after stimulation. Numbers beside boxed areas indicate percentages of cells in S phase. Data are representative of two independent experiments. (**d**) Viability of B cells stimulated with 10 μg/ml of LPS, 1 μM CpG DNA or 10 μg/ml of anti-CD40, as assessed by annexin V staining (time, horizontal axes). Data are representative of three independent experiments. (**e**) ELISA of immunoglobulin isotypes in the sera of unimmunized 8-week-old mice ($n = 10$ mice of each genotype). Each symbol represents one mouse. *, $P < 0.05$ (Student's *t*-test). (**f**) Production of trinitrophenol-specific IgM (TNP-IgM) and IgG3 (TNP-IgG3) at 7 and 14 d after immunization with trinitrophenol-Ficoll. (**g**) Production of nitrophenol-specific IgM (NP-IgM) and IgG1 (NP-IgG1) at 7 and 14 d after immunization with nitrophenol–chicken γ-globulin. Results in **f**,**g** represent three of five mice per genotype; *, $P < 0.05$ (Student's *t*-test). Filled symbols or bars, *Ubc13*$^{+/+}$Cd19-Cre; open symbols or bars, *Ubc13*$^{fl/fl}$Cd19-Cre.

© 2006 Nature Publishing Group http://www.nature.com/natureimmunology

LPS, CpG DNA, anti-IgM and anti-CD40 resulted in slightly defective IκBα degradation but normal NF-κB nuclear translocation in *Ubc13*$^{fl/fl}$Cd19-Cre B cells (**Fig. 4a,b**). Nuclear NF-κB complexes contained similar NF-κB subunits in wild-type and *Ubc13*$^{fl/fl}$Cd19-Cre B cells (**Supplementary Fig. 3** online). In addition, BLP- and CpG DNA–mediated IκBα degradation NF-κB nuclear translocation was indistinguishable in control versus *Ubc13*$^{fl/fl}$LyzsM-Cre bone marrow macrophages (**Fig. 4c,d**). To determine whether Ubc13 is involved in TNFR- and IL-1R-mediated signal transduction, we generated mouse embryonic fibroblasts (MEFs) from control and *Ubc13*$^{fl/fl}$ embryos. Retroviral transduction of Cre into *Ubc13*$^{fl/fl}$ MEFs induced efficient deletion of Ubc13 protein (**Supplementary Fig. 1**). *Ubc13*$^{fl/fl}$ MEFs expressing retroviral Cre had normal TNF- and IL-1β-induced IκBα degradation and NF-κB nuclear translocation (**Fig. 4e,f**). To further investigate whether Ubc13 deficiency is dispensable for NF-κB activation, we transfected an NF-κB-dependent luciferase reporter construct into control or *Ubc13*$^{fl/fl}$ MEFs expressing retroviral Cre. TNF or IL-1β stimulation induced similar luciferase activity in control and *Ubc13*$^{fl/fl}$ MEFs (**Fig. 4g**). Moreover, overexpression of Bcl-10 or CARMA1 resulted in similar NF-κB activation in control and *Ubc13*$^{fl/fl}$ MEFs (**Fig. 4h**). In addition, IL-1β-induced IκBα recovery at later time points was similar for control and *Ubc13*$^{fl/fl}$ MEFs expressing retroviral Cre (**Fig. 4i**). To analyze the function of Ubc13 in alternative pathways of NF-κB activation, we assessed stimulus-dependent processing of the NF-κBp100 subunit. Control and *Ubc13*$^{fl/fl}$Cd19-Cre B cells had similar patterns of processing of NF-κBp100 to NF-κBp52 after stimulation with anti-CD40 or B cell–activating factor of the TNF family (**Supplementary Fig. 3**), indicating that Ubc13 is not involved in the alternative pathway of NF-κB activation. These data collectively suggest that although Ubc13 deficiency slightly affected IκBα degradation in some cell types, Ubc13 seems to be mostly dispensable for NF-κB activation.

Next we investigated activation of the Jnk, p38 and Erk MAP kinases in B cells, bone marrow macrophages and MEFs. Stimulation of control B cells with anti-IgM resulted in phoshorylation of Jnk, p38 and Erk. In contrast, although Erk activation was normal, anti-IgM-induced phoshorylation of Jnk and p38 was substantially impaired in *Ubc13*$^{fl/fl}$Cd19-Cre B cells. Moreover, *Ubc13*$^{fl/fl}$Cd19-Cre B cells had considerably reduced activation of all three MAP kinases in response to LPS and CpG DNA, and anti-CD40-induced MAP kinase activation was also mildly affected by Ubc13 deficiency (**Fig. 5a**). Although stimulation with BLP or CpG DNA resulted in rapid phosphorylation of MAP kinases in control bone marrow macrophages, MAP kinase activation in *Ubc13*$^{fl/fl}$LyzsM-Cre bone marrow macrophages was impaired (**Fig. 5b**). Furthermore, IL-1β-induced phosphorylation of Jnk, p38 and Erk was much lower in *Ubc13*$^{fl/fl}$ than in control MEFs expressing retroviral Cre (**Fig. 5c**). In contrast, TNF stimulation resulted in similar MAP kinase activation in *Ubc13*$^{fl/fl}$ and control MEFs expressing retroviral Cre (**Fig. 5d**). These results collectively demonstrate that Ubc13 is important in MAP kinase activation induced by TLR, IL-1R, BCR and CD40, but not MAP kinase activation induced by TNFR.

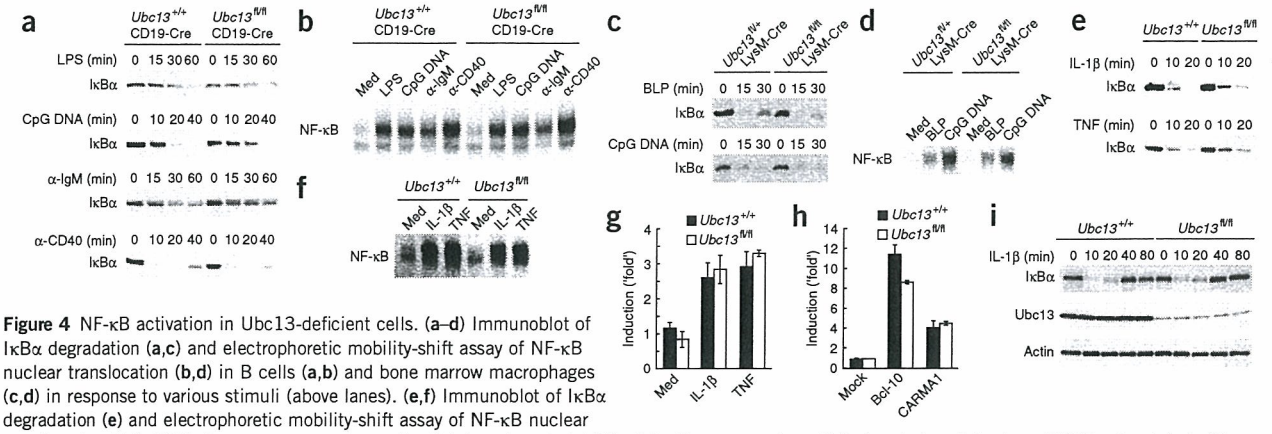

Figure 4 NF-κB activation in Ubc13-deficient cells. (**a–d**) Immunoblot of IκBα degradation (**a**,**c**) and electrophoretic mobility-shift assay of NF-κB nuclear translocation (**b**,**d**) in B cells (**a**,**b**) and bone marrow macrophages (**c**,**d**) in response to various stimuli (above lanes). (**e**,**f**) Immunoblot of IκBα degradation (**e**) and electrophoretic mobility-shift assay of NF-κB nuclear translocation (**f**) in MEFs in response to various stimuli (above lanes). (**g**) NF-κB luciferase reporter activity in whole-cell lysates of MEFs stimulated with 10 ng/ml of IL-1β or 10 ng/ml of TNF. (**h**) NF-κB luciferase reporter activity in whole-cell lysates of MEFs transfected with plasmids encoding Bcl-10 or CARMA1. (**i**) Immunoblot of IκBα degradation and recovery in MEFs stimulated with 10 ng/ml of IL-1β (time, above lanes). Data are representative of two (**i**) or three (**a–h**) independent experiments.

© 2006 Nature Publishing Group http://www.nature.com/natureimmunology

These data indicate that Ubc13 is critically involved in MAP kinase activation, yet has only a minor function in NF-κB activation. To elucidate precisely where in the TLR, IL-1R, BCR and CD40 signaling pathways Ubc13 induces MAP kinase activation, we examined the activation and modification of signaling molecules 'upstream' of the IKK complex and MAP kinase kinase proteins. *In vitro* studies indicate that IL-1β stimulates TRAF6 ubiquitination in a Ubc13-dependent way[16]. Therefore, we examined IL-1β-induced polyubiquitination of TRAF6 in control or *Ubc13*$^{fl/fl}$ MEFs expressing retroviral Cre. IL-1β-induced polyubiquitination of TRAF6 was evident in control and *Ubc13*$^{fl/fl}$ MEFs expressing retroviral Cre (**Fig. 6a**). As the K63-linked ubiquitination of TRAF6 has been linked to activation of the kinase TAK1 (ref. 17), we next examined IL-1β-mediated TAK1 phosphorylation in control and *Ubc13*$^{fl/fl}$ MEFs expressing retroviral Cre. These MEFs had similar amounts of phosphorylated TAK1, albeit with delayed kinetics in *Ubc13*$^{fl/fl}$ MEFs compared with control MEFs (**Fig. 6b**). Next we undertook a biochemical approach in which we added recombinant TRAF6 to extracts from unstimulated control cells, which results in phosphorylation of TAK1 and IKK proteins[16,17] (**Fig. 6c**). The addition of TRAF6 to extracts of *Ubc13*$^{fl/fl}$ MEFs expressing retroviral Cre resulted in slightly impaired TAK1 phosphorylation and normal phosphorylation of IKK proteins. These results suggested that Ubc13 is involved in TAK1 activation but that Ubc13 is not absolutely essential for IL-1β-induced TAK1 activation.

Given that TAK1 is critical in IL-1β-induced activation of NF-κB and MAP kinases[18,19] and that there was considerable activation of TAK1 and NF-κB in *Ubc13*$^{fl/fl}$ MEFs expressing retroviral Cre, TAK1 activation might contribute to the substantial IL-1β-induced NF-κB

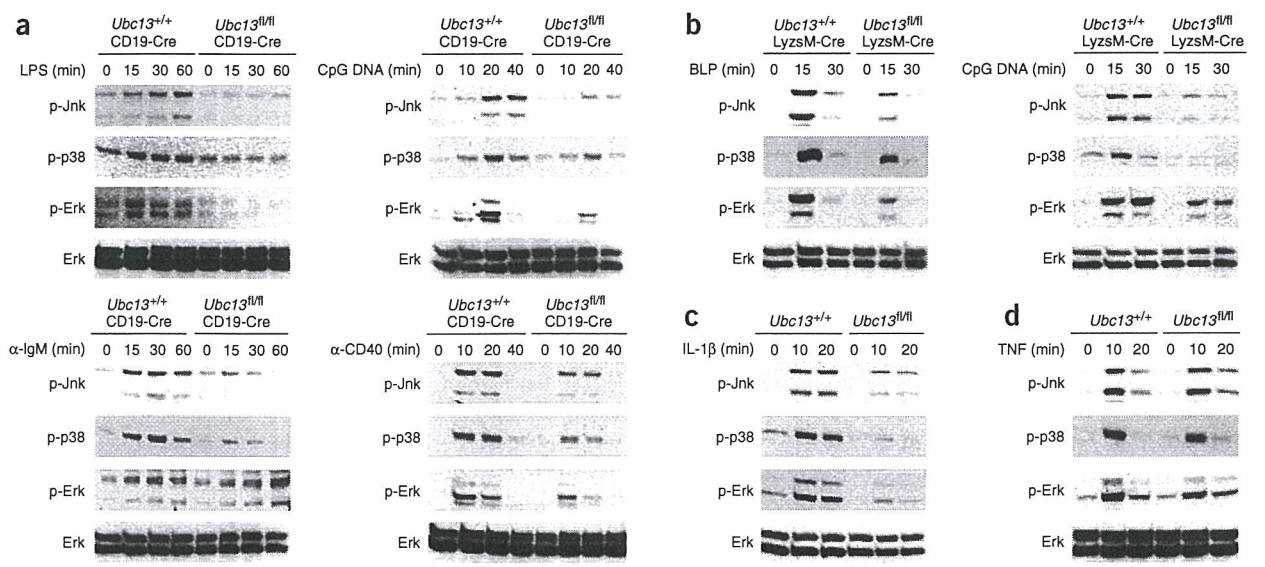

Figure 5 Impaired MAP kinase activation in Ubc13-deficient cells. (**a**) Immunoblot of whole-cell lysates of B cells stimulated with 10 μg/ml of LPS, 1 μM CpG DNA, 10 μg/ml of anti-IgM or 10 μg/ml of anti-CD40. (**b**) Immunoblot of whole-cell lysates of bone marrow macrophages stimulated with 100 ng/ml of BLP or 1 μM CpG DNA. (**c**,**d**) Immunoblot of whole-cell lysates of MEFs stimulated with 10 ng/ml of IL-1β (**c**) or 10 ng/ml of TNF (**d**). p-, phosphorylated. Data are representative of three independent experiments.

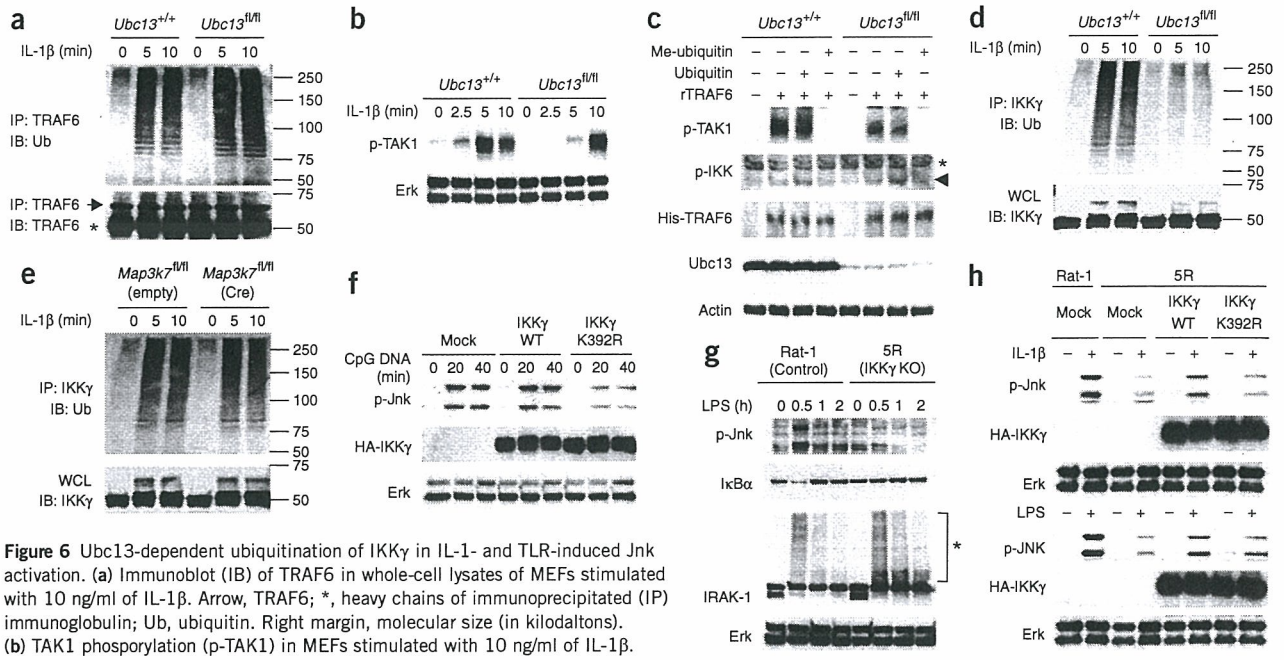

Figure 6 Ubc13-dependent ubiquitination of IKKγ in IL-1- and TLR-induced Jnk activation. (**a**) Immunoblot (IB) of TRAF6 in whole-cell lysates of MEFs stimulated with 10 ng/ml of IL-1β. Arrow, TRAF6; *, heavy chains of immunoprecipitated (IP) immunoglobulin; Ub, ubiquitin. Right margin, molecular size (in kilodaltons). (**b**) TAK1 phosporylation (p-TAK1) in MEFs stimulated with 10 ng/ml of IL-1β. The same lysates were also blotted with anti-Erk1/2 (bottom) to monitor protein expression. (**c**) Immunoblot of cell extracts of MEFs incubated with recombinant TRAF6 (rTRAF6) in the presence of ubiquitin or methylated ubiquitin (Me-ubiquitin). Arrowhead, phosphorylated IKK (p-IKK); *, nonspecific bands; His-, histidine-tagged. (**d**) Immunoblot of IKKγ immunoprecipitates from whole-cell lysates of MEFs stimulated with 10 ng/ml of IL-1β. (**e**) Immunoblot of IKKγ immunoprecipitates from whole-cell lysates of MEFs stimulated with 10 ng/ml of IL-1β. *Map3k7*$^{fl/fl}$, *lox*P-flanked gene encoding TAK1, with (Cre) and without (empty) Cre recombinase. WCL (bottom, **d**,**e**), immunoblot of whole-cell lysates without immunoprecipitation. (**f**) Immunoblot of whole-cell lysates from 70Z/3 pre–B cell lines stably transfected with wild-type (WT) or K392R IKKγ expression vectors. HA-, hemagglutinin-tagged. (**g**) Immunoblot of whole-cell lysates of Rat-1 or 5R cells stimulated with 10 μg/ml of LPS. *, ubiquitinated IRAK-1. (**h**) Immunoblot of whole-cell lysates of Rat-1 or 5R cells stably expressing wild-type or K392R IKKγ expression vectors, stimulated with 10 ng/ml of IL-1β (top) or 10 μg/ml of LPS (bottom). Data are representative of two (**a**,**b**,**d**,**f**,**g**,**h**) or three (**c**,**e**) independent experiments.

© 2006 Nature Publishing Group http://www.nature.com/natureimmunology

activation in the absence of Ubc13. However, given the impaired IL-1β-induced MAP kinase activation in Ubc13-deficient cells, full activation of TAK1 alone may be insufficient for full activation of MAP kinases. Ubc13 has also been suggested to be involved in TCR-induced ubiquitination of IKKγ[15]. We found that IL-1β also stimulated IKKγ polyubiquitination in control MEFs, but that IL-1β-induced IKKγ polyubiquitination was impaired in *Ubc13*$^{fl/fl}$ MEFs expressing retroviral Cre (**Fig. 6d**). Moreover, IL-1β-induced polyubiquitination of IKKγ was normal in TAK1-deficient MEFs (**Fig. 6e**), suggesting that the Ubc13-dependent ubiquitination of IKKγ is a TAK1-independent signaling event.

These aforementioned results prompted us to examine whether the ubiquitination of IKKγ is involved in TLR- and IL-1R-induced MAP kinase activation. As lysine 392 (K392) of mouse IKKγ is known to be the acceptor lysine residue for Ubc13-dependent polyubiquitination[24], we generated a K392R mouse IKKγ mutant and compared CpG DNA–induced Jnk activation in the mouse pre–B cell line 70Z/3 expressing wild-type or K392R IKKγ constructs. The 70Z/3 cells expressing K392R IKKγ had defective activation of Jnk in response to CpG DNA relative to that of mock-transfected 70Z/3 cells or 70Z/3 cells expressing wild-type IKKγ, suggesting that IKKγ K392R inhibits CpG DNA–mediated Jnk activation in a dominant negative way (**Fig. 6f**). Moreover, activation of Jnk and p38 induced by CpG DNA or by phorbol 12-myristate 13-acetate plus ionomycin was impaired in IKKγ-deficient 1.3E2 cells relative to that in control 70Z/3 cells (**Supplementary Fig. 4** online). We further investigated stimulus-dependent activation of MAP kinases in other cell types. MAP kinase activation in response to LPS or IL-1β was reduced considerably in the rat IKKγ-deficient fibroblast cell line 5R as well as in IKKγ-deficient MEFs (**Fig. 6g** and **Supplementary Fig. 4**), indicating that IKKγ is essential for full activation of MAP kinases in response to multiple immune stimuli. To clarify whether ubiquitination of IKKγ is necessary for full MAP kinase activation, we retrovirally expressed wild-type or K392R IKKγ in the IKKγ-deficient 5R fibroblasts and analyzed IL-1β- and LPS-induced Jnk activation. Ectopic expression of wild-type IKKγ induced considerable Jnk activation (**Fig. 6h**). In contrast, K392R IKKγ permitted much weaker Jnk activation. These results indicate that Ubc13-dependent IKKγ ubiquitination may have a partial function in IL-1R- and TLR-induced MAP kinase activation.

DISCUSSION

Here we used a conditional ablation strategy to analyze the physiological function of Ubc13. Ubc13-deficient cells showed almost normal NF-κB activation and severely impaired MAP kinase activation in response to a variety of stimuli, except for TNF. *Ubc13* disruption in bone marrow macrophages resulted in impaired TLR-induced proinflammatory cytokine production and MAP kinase activation. Macrophages treated with MAP kinase inhibitors show defective cytokine production[34,35] and cells lacking MAP kinase phosphatase 5, which show augmented stimulus-dependent Jnk activation, conversely produce increased amounts of cytokines[36], suggesting that MAP kinase activation promotes TLR-induced cytokine production. Failure to activate MAP kinases after TLR stimulation

© 2006 Nature Publishing Group http://www.nature.com/natureimmunology

may have contributed to the reduced cytokine production in Ubc13-deficient bone marrow macrophages. However, there was normal TLR-mediated MyD88-independent expression of type I interferon and interferon-inducible genes in Ubc13-deficient cells, suggesting that Ubc13 is dispensable for TLR-mediated MyD88-independent immune responses.

Ubc13-deficient B cells showed impaired BCR-, CD40- and TLR-mediated activation. In terms of B cell development, mice lacking components of the BCR signaling pathway have phenotypes similar to that of *Ubc13*$^{fl/fl}$Cd19-Cre mice. For example, development of marginal zone B cells and B-1 cells is compromised in *Bcl10*$^{-/-}$ mice and *Malt1*$^{-/-}$ mice[9,13,31]. Although investigation of marginal zone B cells in CARMA1-deficient (*Card11*$^{-/-}$) mice has not been reported, these mice have substantially impaired development of B-1 cells[10–12,14]. Moreover B-1 cell populations are considerably reduced in the peritoneal cavities of mice lacking TAK1, which also participates in BCR signaling[19,37]. Thus, these similarities indicate that Ubc13 may be involved in BCR signaling pathways that are essential for the development of certain B cell lineages. Contrary to published results showing that Ubc13 is involved in TNFR- and TRAF2-dependent activation of NF-κB or MAP kinases[16,28,38], Ubc13-deficient MEFs showed normal TNF-induced activation of NF-κB and MAP kinases, indicating that Ubc13 might have a minor function in TNFR-mediated activation in this cell type.

In response to IL-1β and TLR ligands, Ubc13-deficient cells showed almost normal NF-κB activation and considerable impairment in MAP kinase activation. In addition, there was unexpected IL-1β-induced polyubiquitination of TRAF6 in Ubc13-deficient MEFs. *In vitro* ubiquitination assays in which only Ubc13 and Uev1A E2 ubiquitin ligases are present have shown that TRAF2 and TRAF6 are involved in the generation of K63-linked but not K48-linked polyubiquitin chains[15,16]. However, given that overexpression of TRAF2 *in vivo* generates K63- as well as K48-linked ubiquitination[28], IL-1β-induced Ubc13-independent K48-linked but not Ubc13-dependent K63-linked ubiquitination of TRAF6 might be detected in Ubc13-deficient MEFs. Alternatively, another E2 conjugating enzyme, UbcH7, has been shown to facilitate TRAF6-related K63-linked polyubiquitination[39]. UbcH7 might compensate for the lack of Ubc13 and stimulate IL-1β-induced K63-linked ubiquitination of TRAF6.

Ubc13-dependent ubiquitination is involved in TAK1 activation[17]. Here, Ubc13-deficient MEFs showed almost normal TAK1 phosphorylation, albeit with substantially delayed kinetics, suggesting that Ubc13 is not absolutely required for full activation of TAK1. Analysis of TAK1-deficient cells has demonstrated that TAK1 is essential in TLR- and IL-1R-induced activation of NF-κB and MAP kinases[18,19]. Therefore, we propose that although full TAK1 activation alone may be sufficient to induce considerable NF-κB activation in response to IL-1β, supplemental signaling events 'downstream' of or independent of TAK1 might also be required for the efficient activation of MAP kinases.

Several *in vitro* experiments have demonstrated that IKKγ is ubiquitinated in a Ubc13-dependent way[15,24,27]. In our study here, IL-1β-mediated ubiquitination of IKKγ was considerably impaired in Ubc13-deficient MEFs but was normal in TAK1-deficient cells, suggesting possible involvement of IKKγ ubiquitination in MAP kinase activation. Overexpression of the ubiquitination-deficient K392R IKKγ mutant reduced Jnk activation in 70Z/3 cells. In addition, the derivative IKKγ-deficient cell line 1.3E2 showed defective Jnk and p38 activation in response to CpG DNA (or phorbol 12-myristate 13-acetate plus ionomycin). Indeed, characterization of IKKγ-deficient 1.3E2 cells has demonstrated 'normal' MAP kinase activation in response to stimulation with phorbol 12-myristate 13-acetate plus ionomycin[40]. In contrast, another study has shown that although 1.3E2 cells have impaired Jnk activation in response to the same stimuli tested in that previous study[40], responsiveness is restored by ectopic expression of protein kinase C-θ (PKC-θ), PKC-δ or IKKγ; that study concluded that 1.3E2 cells lack PKC-θ and PKC-δ in addition to PKC-θ and PKC-δ[41]. However, as we reproducibly found impairment in the activation of Jnk and p38 in several IKKγ-deficient cell lines, we believe that IKKγ might be involved in the stimulus-dependent activation of the MAP kinases as well as NF-κB in these cell types. Furthermore, re-expression of the K392R IKKγ mutant, to which K63-linked polyubiquitin chains cannot be appended, in IKKγ-deficient 5R cells conferred much weaker Jnk activation in response to IL-1β and LPS than did wild-type IKKγ, suggesting that Ubc13-dependent IKKγ ubiquitination may be essential at least in part for Jnk activation. The IKKγ-interacting protein Act1 (also called CIKS), whose overexpression potentiates Jnk and NF-κB activation, might be involved in IKKγ-related Jnk activation[42,43]. Studies using Act1-deficient cells may allow examination of that possibility[44].

Although IKKγ deficiency resulted in defective activation of MAP kinases in our study, IKKγ-deficient cell lines may have mutated in the interim between previously published studies and our studies here, resulting in loss of the original phenotype of 'normal' MAP kinase activation reported before[40]. Further analysis using 'knock-in' mice homozygous for the mutation producing the IKKγ K392R substitution will provide physiological conditions in which to examine whether Ubc13-dependent ubiqituitination of IKKγ is involved in the activation of MAP kinases (as well as NF-κB) in response to various stimuli in other cell types and immune responses.

As for the involvement of Ubc13 in NF-κB activation, given that mice lacking either IKKβ or IKKγ, both of which are essential for BCR-induced NF-κB activation, also show defects in the development of marginal zone B cells and B-1 cells[45,46], Ubc13 might be critical to IKKβ-dependent NF-κB activation in a cell type–specific way. Moreover, we cannot exclude the possibility that conditional deletion of Ubc13 may have been incomplete in some cell types or that another E2 family member (such as Ubc5, which is involved in IκBα phosphorylation[47] and K63-linked polyubiquitin chain synthesis[48]) compensated for the loss of Ubc13 in some cell types. Further studies are needed to comprehensively evaluate the function of Ubc13 in NF-κB activation using other cell types such as T cells, hepatocytes and keratinocytes.

In summary, here we have provided genetic evidence that Ubc13 is involved in TLR-, IL-1R-, BCR- and CD40-mediated immune responses in several cell types. We have demonstrated that Ubc13 deficiency 'preferentially' affects the activation of MAP kinases at least in part through induction of ubiquitination of IKKγ. Further studies using conditionally Ubc13-deficient mice may provide a new insight into other Ubc13-dependent, K63-linked, ubiquitination-related biological processes, such as those induced by DNA repair and cellular stress.

METHODS

Generation of *Ubc13*$^{fl/fl}$ mice. Genomic DNA containing *Ubc13* was isolated from a 129/Sv mouse genomic library and was characterized by restriction enzyme mapping and sequencing analysis. The targeting vector was constructed by replacement of a 3.0-kilobase fragment of *Ubc13* with a neomycin-resistance gene cassette. In addition, a 3.0-kilobase fragment of *Ubc13* genomic DNA containing exons 2, 3 and 4 was inserted between two *lox*P sites in the targeting vector pKSTKNEOLOXP, which contains a herpes simplex virus thymidine kinase gene driven by a PGK promoter. The targeting vector was transfected into embryonic stem cells (embryonic day 14.1). Colonies resistant to both G418 and ganciclovir were screened. Homologous recombinants were microinjected into C57BL/6 female mice, and heterozygous F_1 progeny were

intercrossed to generate *Ubc13*$^{fl/fl}$ mice. All animal experiments were done with the approval of the Animal Research Committee of the Research Institute for Microbial Diseases of Osaka University (Osaka, Japan).

Reagents, cells and mice. LPS, poly(I:C), BLP, MALP-2 and CpG oligodeoxynucleotides were prepared as described[42]. Agonistic anti-CD40 and anti-IgM were purchased from PharMingen. B cell–activating factor of the TNF family, IL-1β and TNF were from Genzyme. Antibodies specific for the phosphorylated forms of Erk (9101), Jnk (9251), p38 (9211), IKK (3031) and IκBα (9241) were purchased from Cell Signaling. Antibodies specific for Erk (sc-94), IκBα (sc-371), TRAF6 (sc-7221), IKKγ (sc-8330), ubiquitin (sc-8017), hemagglutinin (sc-3792), histidine (sc-8036), actin (sc-8432) and NF-κBp52 (sc-298) were from Santa Cruz. Monoclonal anti-Ubc13 (37-1100) was from Zymed. Anti-IRAK-1 and anti-phospho-TAK1 have been described[49,50]. The IKKγ-deficient cell line 5R and control cell line Rat-1 (ref. 51), the IKKγ-deficient cell line 1.3E2 and control cell line 70Z/3 (ref. 40), IKK-γ-deficient MEFs[52] and MEFs homozygous for *lox*P-flanked TAK1 and expressing retroviral Cre[19] have been described. Cd19-Cre and LyzsM-Cre mice have been described[53,54].

Preparation of bone marrow macrophages. Bone marrow cells were isolated from femurs and were cultured in RPMI 1640 medium supplemented with 10% FBS and 50 ng/ml of macrophage colony-stimulating factor (R&D Systems). Medium was replaced every 2.5 d. In these conditions, monolayers of adherent cells of which more than 99% expressed surface Mac-1 were obtained. Cells were collected by incubation with 10 mM EDTA in PBS with gentle agitation and were seeded onto plates. After culture for several hours without macrophage colony-stimulating factor, cells were used as bone marrow macrophages.

Measurement of proinflammatory cytokines and electrophoretic mobility-shift assay. These assays were done as described[55].

Purification of B cells and splenic CD4$^+$ T cells. Resting B cells were isolated from splenocyte single-cell suspensions by positive selection with anti-B220 magnetic beads (Miltenyi Biotec). Cell purity was typically more than 97% for B220$^+$ cells, as assessed by flow cytometry.

Plasmids and retroviral transduction. The NF-κB-dependent reporter plasmids and expression vectors containing *Card11* have been described[55,56]. The retroviral vector pMRX encoding Cre protein and the production of retroviruses have been described[19]. At 12 h after infection, 3 μg/ml of puromycin (Invivogen) was added and selected cells were analyzed 48–72 h after infection. Hemagglutinin-tagged wild-type and K392R IKKγ constructs were generated by PCR and were cloned into pMRX retroviral vectors as described[57].

Luciferase reporter assay. This reporter assay was done with the Dual-Luciferase Reporter Assay System (Promega) as described[57].

Immunoblot, immunoprecipitation and *in vivo* ubiquitination assay. After several hours of 'starvation' in DMEM containing 0.1% FBS (to reduce background signal), cells were stimulated with various ligands for various times. Immunoblot and immunoprecipitation were done as described[57]. For detection of *in vivo* ubiquitination of IKKγ and TRAF6, cell lysates were boiled for 10 min at 90 °C in 1% SDS for removal of noncovalently attached proteins, followed by immunoprecipitation with anti-IKKγ or anti-TRAF6 in 0.1% SDS lysis buffer in the presence of protease inhibitors. Ubiquitin was detected by immunoblot anlaysis.

Cell viability assay. Purified splenic B cells (1×10^6) were stimulated with various ligands for various times. Cell viability was assessed with the MEBCYTO Apoptosis kit (MBL) and a FACSCalibur (Becton Dickinson).

Lymphocyte proliferation assay, cell cycle analysis and flow cytometry. These assays were done as described[19].

***In vivo* immunization and enzyme-linked immunosorbent assay (ELISA).** These assays were done as described[19].

Immunohistochemistry. Spleen tissue was embedded in optimum cutting temperature compound (Lab-Tek Products) and was 'flash frozen' in liquid nitrogen. Sections 5 μm in thickness were fixed in cold acetone, were air-dried and were incubated for 1 h at 25 °C in PBS containing 1% BSA, 10% normal rat serum and 5% normal goat serum. Tissue sections were then stained for 60 min at 25 °C with biotin-conjugated anti-mouse CD19 (Pharmingen) followed by streptavidin-conjugated alkaline phosphatase for 30 min, or with rat monoclonal antibody to mouse metallophilic macrophages (MCA947F; Serotec) followed by horseradish peroxidase–conjugated anti-rat. After being stained, sections were washed and were developed with the Vector Blue Alkaline Phosphatase Substrate Kit or the AEC (3-amino-9-ethylcarbazole) Substrate Kit for Horseradish Peroxidase (both from Vector), respectively.

Recombinant TRAF6-inducible *in vitro* system. This *in vitro* system was as described with slight modifications[16,17]. This used TRAF6 cDNA subcloned into pFAST-Bac-HTa (Gibco BRL) for expression in Sf9 insect cells as six-histidine–tagged proteins. Proteins were purified in accordance with the manufacturer's instructions strictly in the absence of EDTA. For detection of phosphorylation of endogenous TAK1 and IKK, cell extracts (3 mg/ml) prepared in reaction buffer (20 mM Tris-HCl, pH 7.5, and 150 mM NaCl; after sonication) were mixed for 2 h at 30 °C with 2 mM ATP, 2 mM $MgCl_2$, 1 mM dithiothreitol and 0.1 M wild-type ubiquitin or 0.1 M methylated ubiquitin in the presence or absence of 0.1 μM recombinant TRAF6. The reaction was terminated by the addition of SDS-PAGE sample buffer, followed by immunoblot analysis with phosphorylation-specific antibodies as described above.

Statistical analysis. We used the unpaired Student's *t*-test to determine the statistical significance of experimental data.

Note: Supplementary information is available on the Nature Immunology website.

ACKNOWLEDGMENTS

We thank T. Kitamura (The University of Tokyo, Tokyo, Japan) for Plat-E packaging cell lines; D.T. Golenbock (University of Massachusetts Medical School, Worcester, Massachusetts) for the NF-κB-dependent ELAM1 reporter plasmid; J.L. Pomerantz (The Johns Hopkins University School of Medicine, Baltimore, Maryland) for *Card11* expression vectors; J. Inoue (The University of Tokyo, Tokyo, Japan) for the pFastBacHTa-TRAF6 vector; G. Courtois (Hôpital Saint-Louis, Paris, France) for the IKKγ-deficient 1.3E2 cell line; M. Pasparakis (European Molecular Biology Laboratory, Rome, Italy) for MEFs from IKKγ-deficient mice; R.C. Rickert (The Burnham Institute, La Jolla, California) for Cd19-Cre mice; I. Förster (University of Munich, Munich, Germany) for LyzsM-Cre mice; H. Hemmi, T. Yasui and T. Matsunaga for discussions; M. Hashimoto for secretarial assistance; and N. Okita, N. Iwami, N. Fukuda and M. Morita for technical assistance. Supported by Special Coordination Funds; the Ministry of Education, Culture, Sports, Science and Technology; Research Fellowships of the Japan Society for the Promotion of Science for Young Scientists; The Uehara Memorial Foundation; The Naito Foundation and The Junior Research Associate from RIKEN; and Exploratory Research for Advanced Technology, Japan Science and Technology Agency.

AUTHOR CONTRIBUTIONS

All authors contributed to data analysis, experimental design, critical discussions and manuscript preparation; M.Y did all experimental studies; T.O. and Y.M. purified recombinant TRAF6; K.T. generated Ubc13-deficient mice; S.S. and S.U. prepared whole-cell extracts; T.S., N.Y. and S.Y. designed retroviral vectors; H.S. prepared antibodies; K.J.I., T.K. and O.T. played a pivotal role in discussions; and S.A. supervised all work.

COMPETING INTERESTS STATEMENT

The authors declare that they have no competing financial interests.

Published online at http://www.nature.com/natureimmunology/
Reprints and permissions information is available online at http://npg.nature.com/reprintsandpermissions/

1. Ghosh, S. & Karin, M. Missing pieces in the NF-κB puzzle. *Cell* **109**, S81–S96 (2002).
2. Weil, R. & Israel, A. T-cell-receptor- and B-cell-receptor-mediated activation of NF-κB in lymphocytes. *Curr. Opin. Immunol.* **16**, 374–381 (2004).
3. Chang, L. & Karin, M. Mammalian MAP kinase signalling cascades. *Nature* **410**, 37–40 (2001).

© 2006 Nature Publishing Group http://www.nature.com/natureimmunology

© 2006 Nature Publishing Group http://www.nature.com/natureimmunology

4. Akira, S. & Takeda, K. Toll-like receptor signalling. *Nat. Rev. Immunol.* **4**, 499–511 (2004).
5. Kobayashi, T., Walsh, M.C. & Choi, Y. The role of TRAF6 in signal transduction and the immune response. *Microbes Infect.* **6**, 1333–1338 (2004).
6. Chung, J.Y., Park, Y.C., Ye, H. & Wu, H. All TRAFs are not created equal: common and distinct molecular mechanisms of TRAF-mediated signal transduction. *J. Cell Sci.* **115**, 679–688 (2002).
7. Lin, X. & Wang, D. The roles of CARMA1, Bcl10, and MALT1 in antigen receptor signaling. *Semin. Immunol.* **16**, 429–435 (2004).
8. Ruland, J. *et al.* Bcl10 is a positive regulator of antigen receptor-induced activation of NF-κB and neural tube closure. *Cell* **104**, 33–42 (2001).
9. Ruland, J., Duncan, G.S., Wakeham, A. & Mak, T.W. Differential requirement for Malt1 in T and B cell antigen receptor signaling. *Immunity* **19**, 749–758 (2003).
10. Jun, J.E. *et al.* Identifying the MAGUK protein Carma-1 as a central regulator of humoral immune responses and atopy by genome-wide mouse mutagenesis. *Immunity* **18**, 751–762 (2003).
11. Hara, H. *et al.* The MAGUK family protein CARD11 is essential for lymphocyte activation. *Immunity* **18**, 763–775 (2003).
12. Egawa, T. *et al.* Requirement for CARMA1 in antigen receptor-induced NF-κB activation and lymphocyte proliferation. *Curr. Biol.* **13**, 1252–1258 (2003).
13. Ruefli-Brasse, A.A., French, D.M. & Dixit, V.M. Regulation of NF-κB-dependent lymphocyte activation and development by paracaspase. *Science* **302**, 1581–1584 (2003).
14. Newton, K. & Dixit, V.M. Mice lacking the CARD of CARMA1 exhibit defective B lymphocyte development and impaired proliferation of their B and T lymphocytes. *Curr. Biol.* **13**, 1247–1251 (2003).
15. Sun, L., Deng, L., Ea, C.K., Xia, Z.P. & Chen, Z.J. The TRAF6 ubiquitin ligase and TAK1 kinase mediate IKK activation by BCL10 and MALT1 in T lymphocytes. *Mol. Cell* **14**, 289–301 (2004).
16. Deng, L. *et al.* Activation of the IκB kinase complex by TRAF6 requires a dimeric ubiquitin-conjugating enzyme complex and a unique polyubiquitin chain. *Cell* **103**, 351–361 (2000).
17. Wang, C. *et al.* TAK1 is a ubiquitin-dependent kinase of MKK and IKK. *Nature* **412**, 346–351 (2001).
18. Shim, J.H. *et al.* TAK1, but not TAB1 or TAB2, plays an essential role in multiple signaling pathways *in vivo. Genes Dev.* **19**, *2668–2681 (2005).*
19. Sato, S. *et al.* Essential function for the kinase TAK1 in innate and adaptive immune responses. *Nat. Immunol.* **6**, 1087–1095 (2005).
20. Spence, J., Sadis, S., Haas, A.L. & Finley, D. A ubiquitin mutant with specific defects in DNA repair and multiubiquitination. *Mol. Cell. Biol.* **15**, 1265–1273 (1995).
21. Pickart, C.M. & Fushman, D. Polyubiquitin chains: polymeric protein signals. *Curr. Opin. Chem. Biol.* **8**, 610–616 (2004).
22. Hofmann, R.M. & Pickart, C.M. Noncanonical MMS2-encoded ubiquitin-conjugating enzyme functions in assembly of novel polyubiquitin chains for DNA repair. *Cell* **96**, 645–653 (1999).
23. Muralidhar, M.G. & Thomas, J.B. The *Drosophila* bendless gene encodes a neural protein related to ubiquitin-conjugating enzymes. *Neuron* **11**, 253–266 (1993).
24. Zhou, H. *et al.* Bcl10 activates the NF-κB pathway through ubiquitination of NEMO. *Nature* **427**, 167–171 (2004).
25. Zhou, R. *et al.* The role of ubiquitination in *Drosophila* innate immunity. *J. Biol. Chem.* **280**, 34048–34055 (2005).
26. Andersen, P.L. *et al.* Distinct regulation of Ubc13 functions by the two ubiquitin-conjugating enzyme variants Mms2 and Uev1A. *J. Cell Biol.* **170**, 745–755 (2005).
27. Zhou, H., Du, M.Q. & Dixit, V.M. Constitutive NF-κB activation by the t(11;18)(q21;q21) product in MALT lymphoma is linked to deregulated ubiquitin ligase activity. *Cancer Cell* **7**, 425–431 (2005).
28. Habelhah, H. *et al.* Ubiquitination and translocation of TRAF2 is required for activation of JNK but not of p38 or NF-κB. *EMBO J.* **23**, 322–332 (2004).
29. Kobayashi, N. *et al.* Segregation of TRAF6-mediated signaling pathways clarifies its role in osteoclastogenesis. *EMBO J.* **20**, 1271–1280 (2001).
30. Gohda, J., Matsumura, T. & Inoue, J. Cutting edge: TNFR-associated factor (TRAF) 6 is essential for MyD88-dependent pathway but not toll/IL-1 receptor domain-containing adaptor-inducing IFN-β (TRIF)-dependent pathway in TLR signaling. *J. Immunol.* **173**, 2913–2917 (2004).
31. Xue, L. *et al.* Defective development and function of Bcl10-deficient follicular, marginal zone and B1 B cells. *Nat. Immunol.* **4**, 857–865 (2003).
32. Hayden, M.S. & Ghosh, S. Signaling to NF-κB. *Genes Dev.* **18**, 2195–2224 (2004).
33. Chen, Z.J. Ubiquitin signalling in the NF-κB pathway. *Nat. Cell Biol.* **7**, 758–765 (2005).
34. Carter, A.B., Monick, M.M. & Hunninghake, G.W. Both Erk and p38 kinases are necessary for cytokine gene transcription. *Am. J. Respir. Cell Mol. Biol.* **20**, 751–758 (1999).
35. Scherle, P.A. *et al.* Inhibition of MAP kinase kinase prevents cytokine and prostaglandin E2 production in lipopolysaccharide-stimulated monocytes. *J. Immunol.* **161**, 5681–5686 (1998).
36. Zhang, Y. *et al.* Regulation of innate and adaptive immune responses by MAP kinase phosphatase 5. *Nature* **430**, 793–797 (2004).
37. Shinohara, H. *et al.* PKC beta regulates BCR-mediated IKK activation by facilitating the interaction between TAK1 and CARMA1. *J. Exp. Med.* **202**, 1423–1431 (2005).
38. Shi, C.S. & Kehrl, J.H. Tumor necrosis factor (TNF)-induced germinal center kinase-related (GCKR) and stress-activated protein kinase (SAPK) activation depends upon the E2/E3 complex Ubc13-Uev1A/TNF receptor-associated factor 2 (TRAF2). *J. Biol. Chem.* **278**, 15429–15434 (2003).
39. Geetha, T., Kenchappa, R.S., Wooten, M.W. & Carter, B.D. TRAF6-mediated ubiquitination regulates nuclear translocation of NRIF, the p75 receptor interactor. *EMBO J.* **24**, 3859–3868 (2005).
40. Courtois, G., Whiteside, S.T., Sibley, C.H. & Israel, A. Characterization of a mutant cell line that does not activate NF-κB in response to multiple stimuli. *Mol. Cell. Biol.* **17**, 1441–1449 (1997).
41. Krappmann, D., Patke, A., Heissmeyer, V. & Scheidereit, C. B-cell receptor- and phorbol ester-induced NF-κB and c-Jun N-terminal kinase activation in B cells requires novel protein kinase C's. *Mol. Cell. Biol.* **21**, 6640–6650 (2001).
42. Leonardi, A., Chariot, A., Claudio, E., Cunningham, K. & Siebenlist, U. CIKS, a connection to IκB kinase and stress-activated protein kinase. *Proc. Natl. Acad. Sci. USA* **97**, 10494–10499 (2000).
43. Li, X. *et al.* Act1, an NF-κB-activating protein. *Proc. Natl. Acad. Sci. USA* **97**, 10489–10493 (2000).
44. Qian, Y. *et al.* Act1, a negative regulator in CD40- and BAFF-mediated B cell survival. *Immunity* **21**, 575–587 (2004).
45. Pasparakis, M., Schmidt-Supprian, M. & Rajewsky, K. IκB kinase signaling is essential for maintenance of mature B cells. *J. Exp. Med.* **196**, 743–752 (2002).
46. Li, Z.W., Omori, S.A., Labuda, T., Karin, M. & Rickert, R.C. IKKβ is required for peripheral B cell survival and proliferation. *J. Immunol.* **170**, 4630–4637 (2003).
47. Chen, Z. *et al.* Signal-induced site-specific phosphorylation targets IκBα to the ubiquitin-proteasome pathway. *Genes Dev.* **9**, 1586–1597 (1995).
48. Duncan, L.M. *et al.* Lysine-63-linked ubiquitination is required for endolysosomal degradation of class I molecules. *EMBO J.* **25**, 1635–1645 (2006).
49. Yamamoto, M. *et al.* Role of adaptor TRIF in the MyD88-independent toll-like receptor signaling pathway. *Science* **301**, 640–643 (2003).
50. Singhirunnusorn, P., Suzuki, S., Kawasaki, N., Saiki, I. & Sakurai, H. Critical roles of threonine 187 phosphorylation in cellular stress-induced rapid and transient activation of transforming growth factor-β-activated kinase 1 (TAK1) in a signaling complex containing TAK1-binding protein TAB1 and TAB2. *J. Biol. Chem.* **280**, 7359–7368 (2005).
51. Yamaoka, S. *et al.* Complementation cloning of NEMO, a component of the IκB kinase complex essential for NF-κB activation. *Cell* **93**, 1231–1240 (1998).
52. Schmidt-Supprian, M. *et al.* NEMO/IKKγ-deficient mice model incontinentia pigmenti. *Mol. Cell* **5**, 981–992 (2000).
53. Rickert, R.C., Roes, J. & Rajewsky, K. B lymphocyte-specific, Cre-mediated mutagenesis in mice. *Nucleic Acids Res.* **25**, 1317–1318 (1997).
54. Clausen, B.E., Burkhardt, C., Reith, W., Renkawitz, R. & Forster, I. Conditional gene targeting in macrophages and granulocytes using *LysM*cre mice. *Transgenic Res.* **8**, 265–277 (1999).
55. Yamamoto, M. *et al.* TRAM is specifically involved in the Toll-like receptor 4-mediated MyD88-independent signaling pathway. *Nat. Immunol.* **4**, 1144–1150 (2003).
56. Pomerantz, J.L., Denny, E.M. & Baltimore, D. CARD11 mediates factor-specific activation of NF-κB by the T cell receptor complex. *EMBO J.* **21**, 5184–5194 (2002).
57. Yamamoto, M. *et al.* Regulation of Toll/IL-1-receptor-mediated gene expression by the inducible nuclear protein IκBζ. *Nature* **430**, 218–222 (2004).

Chromatin immunoprecipitation-mediated target identification proved aquaporin 5 is regulated directly by estrogen in the uterus

Mika Kobayashi, Eri Takahashi, Shin-ichi Miyagawa, Hajime Watanabe* and Taisen Iguchi

Okazaki Institute for Integrative Bioscience, National Institutes of Natural Sciences, 5-1 Higashiyama, Myodaiji, Okazaki, 444-8787, Japan

Estrogens play a central role in the reproduction of vertebrates and affect a variety of biological processes. The major target molecules of estrogens are nuclear estrogen receptors (ERs), which have been studied extensively at the molecular level. In contrast, our knowledge of the genes that are regulated directly by ERs remains limited, especially at the level of the whole organism rather than cultured cells. In order to identify genes that are regulated directly by ERs *in vivo*, we used estrogen treated mouse uterus and performed chromatin immunoprecipitation. Sequence analysis of a precipitated DNA fragment enabled alignment with the mouse genomic sequence and revealed that the promoter region of the gene encoding aquaporin 5 (*AQP5*) was precipitated with antibody against ERα. Quantitative PCR and DNA microarray analyses confirmed that *AQP5* is activated soon after administration of estrogen. In addition, the promoter region of *AQP5* contained a functional estrogen response element that was activated directly by estrogen. Although several *AQP* genes are expressed in the uterus, only direct activation of *AQP5* could be detected following treatment with estrogen. This chromatin immunopreciptation-mediated target identification may be applicable to the study of other transcription factor networks.

Introduction

Estrogens play crucial roles in reproduction and other biological processes via two pathways. Firstly, they exert their effects genomically through the estrogen receptors (ERs), which function as ligand-dependent transcription factors that bind DNA at conserved estrogen response elements (EREs). Two ERs (ERα and ERβ) have been identified in mammals and since ERα knockout mice are sterile, the former is considered to play an essential role in reproduction (Lubahn *et al.* 1993). Secondly, estrogens function in a non-genomic manner by rapid activation of membrane-initiated kinase cascades such as the MAPK (Migliaccio *et al.* 1996) and phosphatidylinositol-3-OH kinase (Simoncini *et al.* 2000) signaling pathways. As the net effect of estrogen represents the integration of both genomic and non-genomic activities (Kahlert *et al.* 2000; Wong *et al.* 2002), it is important to distinguish between these pathways when attempting to understand its functions.

Communicated by: Hiroshi Handa

**Correspondence*: E-mail: watanabe@nibb.ac.jp

Membrane binding assays (Inoue *et al.* 1993), computational analyses (Bourdeau *et al.* 2004; Kamalakaran *et al.* 2005) and chromatin immunoprecipitation (ChIP) (Carroll *et al.* 2005; Laganiere *et al.* 2005) have been used to identify ER target genes in a non-biased manner. In particular, the recently developed ChIP technique has enabled investigation of genes at a genome-wide level. However, these approaches have been applied primarily to cultured cell lines such as MCF-7. Consequently, the estrogen target genes of whole organisms remain poorly understood in comparison to cultured cell lines.

The uterus is known to be a major target organ for estrogen and its condition both physiologically and morphologically depends upon estrogen levels. ERα is expressed at high levels in the uterus and in ERα knockout mice the effects of estrogen are canceled. From studies using ERα and ERβ null mice (Lubahn *et al.* 1993; Krege *et al.* 1998), it is known that the former plays an essential role in reproduction.

Although the influence of estrogen on the uterus is both well recognized and studied, our understanding of estrogen-activated transcriptional networks remains limited. Several groups have examined the uterine gene

DOI: 10.1111/j.1365-2443.2006.01009.x

© 2006 The Authors
Journal compilation © 2006 by the Molecular Biology Society of Japan/Blackwell Publishing Ltd.

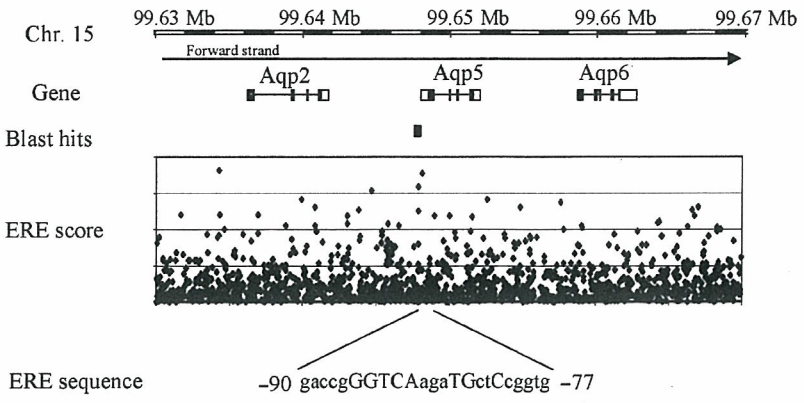

Figure 1 Genome map around *AQP5*. The solid box below the mouse genome map indicates the region identified by BLAST as matching the DNA fragment precipitated by anti-ERα antibody. The locations of *AQP2*, *AQP5* and *AQP6* are mapped on chromosome 15, with exons and flanking regions indicated by solid black and open boxes, respectively. ERE scores were calculated using the PATSER program (Hertz & Stormo 1999), and the putative ERE sequence in the 5′ flanking region of *AQP5* is indicated.

expression profile (Watanabe *et al.* 2002; Hewitt *et al.* 2003; Moggs *et al.* 2004), but none have determined whether these genes were activated directly by ER. Thus, it is not clear to what extent these genes are activated as a direct result of genomic action by estrogen in the target organ.

One of the prominent effects of estrogen is water imbibition in the uterine endometrium. This estrogen-stimulated water transport is considered to be important in the periimplantation period to change the uterine environment. For the regulation of water transportation, water channels termed aquaporins (AQP) play a critical role. AQPs are a family of transmembrane channel proteins that have six transmembrane domains. Thirteen AQPs (AQP0–AQP12) have been identified in mammals and the expression of AQPs in the uterus has also been studied at the protein and RNA level (Offenberg *et al.* 2000; Jablonski *et al.* 2003; Richard *et al.* 2003), although there has not been a study to address whether the AQP genes could be directly activated by estrogen.

In order to identify the genes that are regulated directly by estrogen in the whole organism, we used ChIP to select activated genes in the mouse uterus. A DNA fragment that was recognized by the ER was precipitated and identified as the 5′ region flanking *AQP5*. We analyzed its function and response to estrogen as well as the responses of other *AQP* genes.

Results

AQP5 is a target of ERα

We used ChIP to investigate the uterine genes targeted by ERα. The mouse uterus was fixed 1 h after estrogen treatment, after which genomic DNA was fragmented and precipitated using anti-ERα antibody. This DNA was amplified by PCR and sequenced and compared to the mouse genome. One of the sequences of a precipitated DNA fragment mapped to Chr:15 99647562-99647991, located only 6 bases upstream of *AQP5* (Chr:15 99,647,997-99 652 041; Fig. 1). In contrast, no specific DNA fragments that could be assigned to mouse genome sequence were recovered from ChIP of the untreated uterus (data not shown).

Although a canonical ERE was not identified in the precipitated sequence, a highly conserved motif was found upstream of *AQP5* (between −85 and −73; Fig. 1). To confirm binding of ERα to the putative ERE, we performed a conventional ChIP with fragments from the 5′ flanking and coding regions of *AQP5* (Fig. 2A and Table 1). Only fragments containing the putative ERE and its adjacent sequences could be precipitated following administration of estrogen (Fig. 2B). The other fragments could not be precipitated with anti-ERα antibody, even after administration of E2. Similar results could be

Table 1 Primer sequences used for ChIP analysis of *AQP5*

Primer set	Position	Direction	Primer sequence
1	−1885	F	AATCTGCTTGTCTCTGCCTC
	−1691	R	CCTTCTCTTTCCCAGCTAAC
2	−946	F	GACAAGAGGAAGCTGGGAAC
	−818	R	CCGGCCTATCTCACTTTCTA
3	−506	F	GAAAGACCAACAGGGACAAG
	−318	R	TTCTCAGTGGTAGCCCTTGG
4	−338	F	CCCAAGGGCTACCACTGAGA
	−101	R	ACGGACGGGTCAGAGTGATG
5	−161	F	GGGCGGATAAGGAGCTAAGA
	76	R	GTGCGTGCTGGGCTCTCCTG
6	1026	F	CCTGGCTTCTCTTCACATTC
	1228	R	GTTGCTCCAGACCTCCATCC
7	1996	F	CTCCCCAGCCTTATCCATTG
	2269	R	GTCTCTGTGCTCGCCCTCCC

© 2006 The Authors
Journal compilation © 2006 by the Molecular Biology Society of Japan/Blackwell Publishing Ltd.

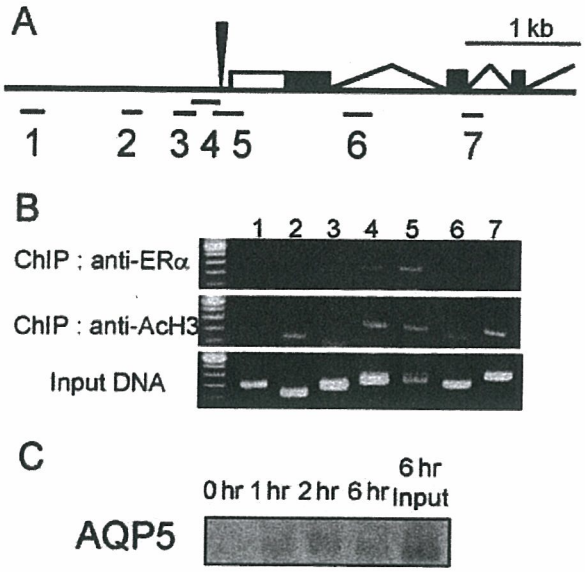

Figure 2 ChIP of the 5′ flanking region of *AQP5*. (A) Schematic of the 5′ region of *AQP5*. The transcriptional initiation site and exons are indicated by an arrowhead and solid black boxes, respectively. Numbered bars indicate the genomic regions examined by PCR following ChIP. (B) ChIP analysis of the 5′ region of *AQP5*. ChIP was performed using either anti-ERα or anti-acetylated histone H3 antibodies, on samples of uterine tissue that were prepared 1 h after the administration of estrogen. Precipitated DNA fragments were amplified by PCR and the lane numbers correspond to the location of the PCR products indicated in (A). The presence of a PCR product indicates precipitation of a DNA fragment by the specified antibody. (C) Temporal analysis of binding between ERα and the *AQP5* promoter region. ChIP was performed on uterine tissue samples harvested 0, 1, 2 and 6 h following administration of estrogen. DNA fragments were precipitated with anti-ERα antibody, then amplified by PCR using primers for the ERE region (#4 in Fig. 2A). The presence of a PCR product indicates binding between ERα and the *AQP5* promoter region.

obtained with monoclonal anti-ERα antibodies. These results suggest that the putative ERE plays a key role in the estrogen response. In contrast, all DNA fragments could be precipitated with anti-acetylated histone H3 antibody (anti-AcH3). It is known that the modification states of the N-terminal tails of hitones H3 and H4 play important role in chromatin formation (Richards & Elgin 2002) and the fact that Lys9 of H3 was acetylated indicated that the chromatin state of the 5′ flanking region of *AQP5* was active.

We examined the temporal changes in binding between ERα and the putative ERE following administration of estrogen. Binding could be detected 1 h after estrogen administration and continued for at least 6 h (Fig. 2C). In contrast, no PCR product was detected from samples precipitated with IgG (data not shown).

Identification of an ERE in the 5′ flanking region of AQP5

In order to determine whether the putative ERE plays a functional role in estrogen-dependent transcriptional activation, we used three luciferase reporter constructs (p611AQP5-luc, p103AQP5-luc and p13AQP5-luc) containing deletions of the 5′ flanking region of *AQP5* (−611, −103 and −13 to +74, respectively).

Only the positive control (containing 3 × canonical ERE) and the two constructs containing the putative ERE (p611AQP5-luc and p103AQP5-luc) were activated by estrogen, whereas the construct that did not contain the putative ERE (p13AQP5-luc) and a construct in which the element was mutated (pm103AQP5-luc; GGTCA→aaTCA), were unaffected (Fig. 3). These results suggest that there is a functional ERE element in the 5′ region of *AQP5* that is regulated directly by ERα.

DNA microarray analysis

In order to obtain a uterine gene expression profile following treatment with estrogen, and to identify gene targets that were regulated directly by ERα rather than via secondary effects of estrogen, we performed a DNA microarray analysis of mouse uterus isolated 1 h following treatment. At 1 h following administration of estrogen, we identified a more than twofold up- or down-regulation in 216 and 204 genes, respectively. As *AQP5* is located between *AQP2* and *AQP6*, we examined whether other *AQP* genes were affected by estrogen. At 1 h post-treatment, expression of *AQP5* and *AQP8* was activated, whereas expression of the *AQP* genes in the proximity of the former (*AQP2* and *AQP6*) was unaffected (Fig. 4).

Quantitative PCR analysis of AQP genes

As the DNA microarray indicated early activation of *AQP5* and *AQP8* by estrogen, we examined temporal expression changes of all AQP genes using quantitative PCR, because it has been reported several AQP genes are expressed in uterus and spatiotemporally regulated during the periimplantation (Richard *et al.* 2003). We confirmed that *AQP5* and *AQP8* were activated within 1 h of estrogen administration and that activation continued for at least 2 h. Although *AQP5* activation declined after 6 h relative to untreated samples, the levels of transcript remained elevated at 24 h (Fig. 5). The other *AQP* genes, including *AQP2* and *AQP6*, were not activated by estrogen.

© 2006 The Authors
Journal compilation © 2006 by the Molecular Biology Society of Japan/Blackwell Publishing Ltd.

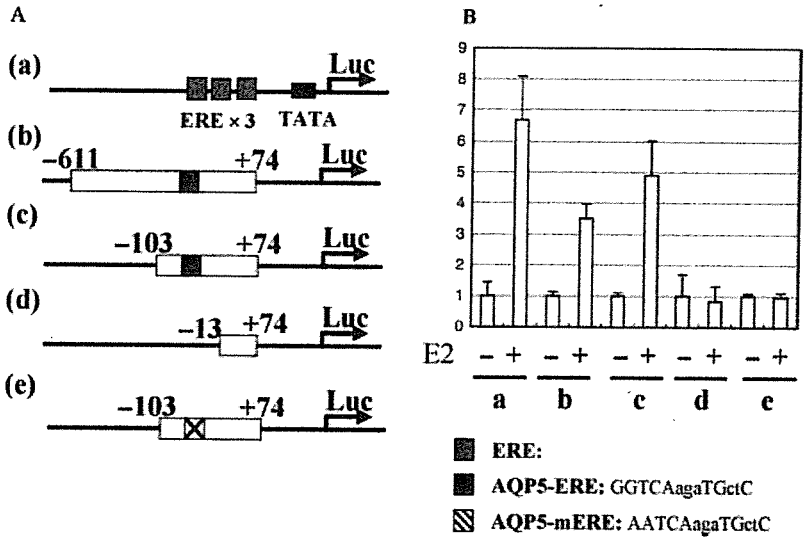

Figure 3 Presence of a functional ERE in the 5′ flanking region of *AQP5*. (A) Luciferase reporter constructs. The positive control (a) contained three canonical ERE elements. Three constructs contained deletions of the 5′ flanking region of *AQP5* (b) p611AQT5-luc, (c) p103AQT5-luc, and (d) p13AQP5-luc and one contained a mutation of the putative ERE sequence (e) pm103AQP5-luc. Black boxes indicate the presence of a putative ERE motif in the *AQP5* promoter region (-86GGTCAagaTGctC-74). Crossed boxes indicate a mutation in the putative ERE motif (AATCAagaTGctC). Gray boxes indicate the canonical ERE motif used as a positive control. (B) The response of 5′ flanking regions of *AQP5* to estrogen stimulation. Luciferase reporter constructs were transfected into HEK293 cells with an ERα expression vector and a control plasmid, then examined in the presence or absence of estrogen. Luciferase intensities detected in the presence of estrogen were divided by those in the absence of estrogen and the relative differences calculated.

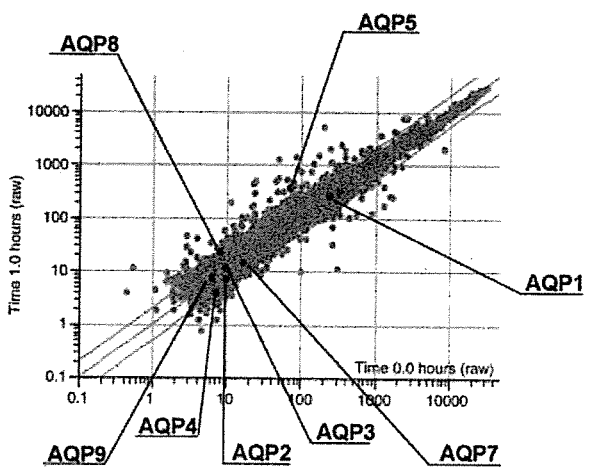

Figure 4 DNA microarray analysis of the expression profile of *AQP* genes. Gene expression levels (intensity of fluorescence) of *AQP* genes determined 1 h after the administration of estrogen (*x*-axis) compared with those at 0 h (*y*-axis). *AQP* genes on the DNA microarray are indicated.

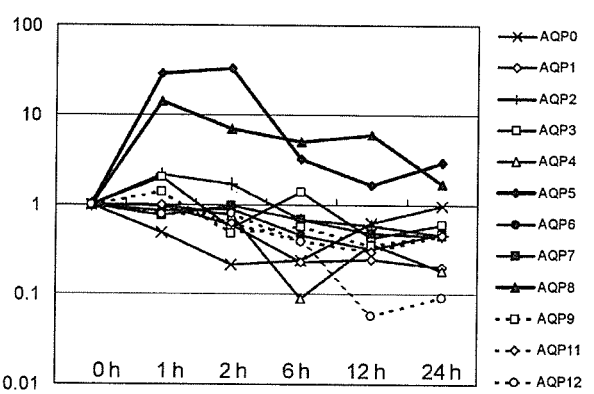

Figure 5 Temporal changes in expression of *AQP* genes following estrogen treatment. Total RNAs were prepared from mouse uteri at 0, 1, 2, 6, 12 and 24 h following estrogen administration, and expression levels of *AQP* genes were estimated using quantitative PCR. Changes relative to expression at 0 h are indicated using a log scale.

© 2006 The Authors
Journal compilation © 2006 by the Molecular Biology Society of Japan/Blackwell Publishing Ltd.

Table 2 ERE-like motifs identified in the promoter regions of *AQP* genes and primer sequences for ChIP analysis of *AQP* genes

Gene	Position	Putative ERE sequence	Score	Position	Direction	ChIP primer sequence
AQP1	−348/−330	TCAGGCAcCCTTGAgCTTT	72	−467	F	TCAGAGTGGGATGGGACAGG
	−810/−828	GAAtGACAGCTgGACCTGA	72	−296	R	GGCCAGAGAAATCCAGGTGT
AQP2	−327/−355	GCtGtGTcCAGTGACCTTC	72	−430	F	CAGAAGAAAGACCATCCAGT
				−268	R	CCAGCCCCCACAATGACCAC
AQP3	−581/−563	TCcAGACgGTGTGACCaGG	76	−617	F	AAGGAGAAAGCCCAGGTATC
				−355	R	TGCGATGACTGGATAGAACA
AQP4	–			−174	F	CTGAAATGCCCTGTGTCTAT
				37	R	AGCTCTGTCACTCATGCCTT
AQP5	−123/−105	TCtcaTCACTCTGACCCGT	78	−163	F	GGGCGGATAAGGAGCTAAGA
	−70/−88	CCgGaGCATCTTGACCCGG	78	74	R	GTGCGTGCTGGGCTCTCCTG
AQP6	−843/−825	AAgAGGCACGGTGACaCTT	70	−945	F	CCAGGTGCAGCCAGGGTTAG
				−748	R	CTTCGGGACCTTGTTCTCAG
AQP7	−714/−696	TCAGcTCcCTCTGACCTCA	83	−751	F	CTGAACCCAGACAAACCATT
				−602	R	TAGGAAAAGTATGCCCAAGG
AQP8	−490/−472	TGcAGGCAGTGTGAgCaGA	71	−569	F	TGCCGATGAAACAGTGAAAG
	−571/−553	AAcAGTGAAAGTGACtCGA	71	−419	R	GACCTACGGGCTTACCTACC
AQP9	+22/+4	ATtAGGAACTGTGACtTAA	72	−57	F	GCAAACAAATAGCAATGAGC
				74	R	ATCTCTGGAGGCGACTAAAG
AQP11	−717/−735	ATtGGGCACCTTtACCTGC	74	−199	F	CGGAGTGTGCAAAGATCAAG
				17	R	AGGGGACAACGGTCTGTAGA
AQP12	−92/−74	ACttGGCtCTGTGACCaAT	76	−105	F	TCCTCTGTGGGTGTTCCTTG
				79	R	TCAGTCTGGGTTCTACAAGG
consensus		NNARGNNANNNTGACCYNN				

The highest-scoring putative ERE-like motifs that were identified in the 5′ flanking regions (within 1 kb) of *AQP* genes (Heinemeyer *et al.* 1999).

Although uterine expression of *AQP* genes has been examined by other groups at the protein and RNA levels, not all of these observations were in agreement. Weak ERE motifs were found in a proximal promoter region (< 1 kb) upstream of *AQP8* and similar motifs were identified upstream of other *AQP* genes (Table 2). Thus, we examined whether the motifs upstream of the various *AQP* genes were functional EREs.

Using a reporter system, we examined whether the regions flanking the *AQP* genes could respond to estrogen stimulation. We prepared transcriptional fusions comprising 1 kb of sequence upstream of each *AQP* gene and the gene encoding luciferase. With the exception of *AQP5*, no *AQP* genes were activated by estrogen (Fig. 6), including *AQP8*, which had been activated by the administration of estrogen in earlier experiments (Figs 4 and 5).

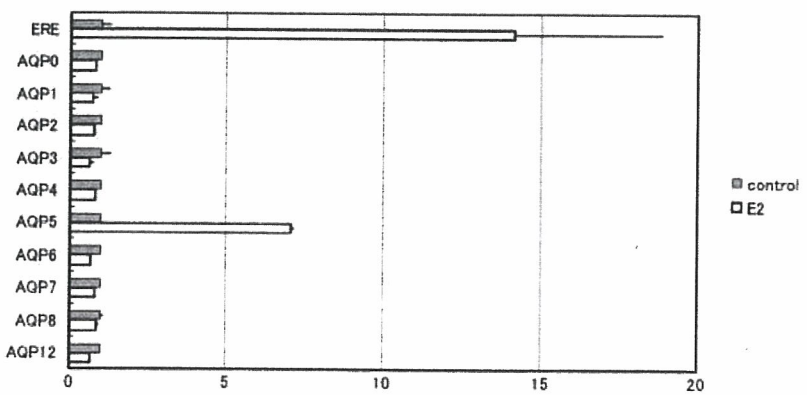

Figure 6 Luciferase reporter assay of *AQP* genes. Estrogen activation of *AQP* genes was examined using luciferase reporter constructs containing the 5′ flanking region of each gene. The luciferase activities of constructs in the presence (open) or absence (gray) of estrogen are indicated relative to a control reporter. ERE indicates the positive control containing three repeats of a canonical ERE motif.

© 2006 The Authors
Journal compilation © 2006 by the Molecular Biology Society of Japan/Blackwell Publishing Ltd.

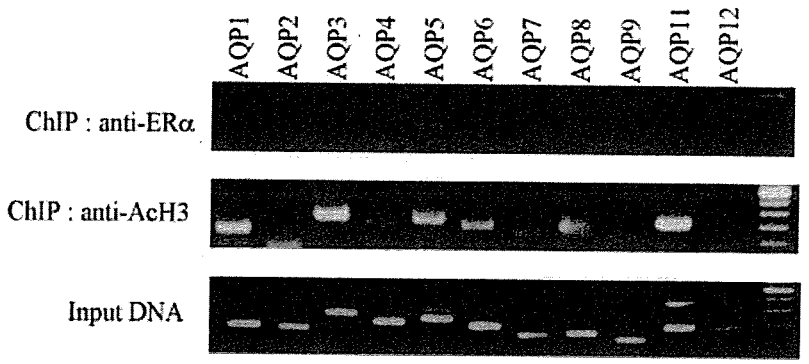

Figure 7 ChIP of the 5′ flanking regions of *AQP* genes. ChIP was performed using either anti-ERα or anti-acetylated histone H3 antibodies, on samples of uterine tissue that were prepared 1 h after administration of estrogen. Precipitated DNA fragments were amplified by PCR using primers (Table 1) designed to amplify the putative EREs (Table 3) of each *AQP* gene.

Next, in order to examine if weak EREs might be recognized by ERα in the uterus, we performed a chromatin immunoprecipitation using anti-ERα. PCR primers were designed to amplify putative ERE sequences in the 5′ flanking region of each *AQP* gene (Table 2). As the only DNA fragment that could be amplified by PCR contained the ERE of *AQP5* (Fig. 7), these results suggest that ERα cannot bind to the flanking region of other *AQP* genes, although some other AQPs have half ERE (AQP2,3,7, and 12).

Discussion

Methodology

In this study, we identified *AQP5* as an ERα target gene through a combination of ChIP and DNA microarray analysis. Previously, we identified hundreds of genes in the mouse uterus that were activated by exposure to estrogen (Watanabe *et al.* 2002), but it was not clear whether those genes were activated directly by estrogen via ERα. We have identified a direct target of ERα using chromatin immunoprecipitation and DNA microarray analysis, and this methodology can be applied to other transcription factors, including other nuclear receptors.

Identification of the target genes of transcription factors is critical to our understanding of transcriptional networks. For example, as canonical EREs were rarely found in promoter regions (O'Lone *et al.* 2004), it was difficult to identify the target genes of ERs by sequence motifs alone; filter binding (Inoue *et al.* 1993), computational approaches (Bourdeau *et al.* 2004; Kamalakaran *et al.* 2005) and ChIP on Chip (Carroll *et al.* 2005; Laganiere *et al.* 2005) have been applied to their identification. As these studies focused primarily on cultured cells, no information regarding whole organisms was available. Previously, we demonstrated the differential expression of estrogen response genes between tissues and throughout various stages of maturation (Watanabe *et al.* 2004). Thus, identification of the direct gene targets of ERα in whole organisms will contribute to our understanding of the function of estrogen during development and maturation.

Although transcription factor binding sites can be determined using ChIP on Chip, this technique requires a large set of arrays, whereas our study did not. A recent report described the use of ChIP with a paired-end ditag sequencing strategy (Wei *et al.* 2006) and this technique may be useful for increasing the numbers of known binding sites and obtaining a genome-wide perspective.

We were unable to estimate the amount of nonspecific contamination of DNA fragments that occurred with the ChIP procedure because it was not possible to map any of the fragments precipitated from the untreated uterus, a result that suggests that our protocol had a very low background. In order to reduce background we introduced a density gradient to remove uncoupled DNA fragments prior to immunoprecipitation. In addition, we introduced steps such as perfusion of the mouse tissue, sonication, and washing of the bound samples, all of which contributed to the reduced background.

Previously, we investigated the temporal regulation of uterine genes by estrogen (Watanabe *et al.* 2003), but were unable to distinguish whether the activation was a direct effect of ERα or a secondary effect of estrogen. In combination with the results from ChIP, previous DNA microarray data may now be interpreted in greater detail.

Aquaporin in the uterus

The effect of estrogen can be observed clearly in the uterine response. Within 1–2 h of estrogen administration, uterine wet weight begins to increase via water imbibition. Although vascular endothelial growth factors are considered to be crucial to this process (Cullinan-Bove & Koos 1993), the contribution of actual water channels

© 2006 The Authors
Journal compilation © 2006 by the Molecular Biology Society of Japan/Blackwell Publishing Ltd.

(AQPs) remains poorly understood. However, AQPs are considered to play an important role in the periimplantation stage and it is known that *AQP1,4* and *5* are expressed at that stage (Li *et al.* 1994; Jablonski *et al.* 2003; Richard *et al.* 2003; Lindsay & Murphy 2004).

In this study, we demonstrated that ERα regulates *AQP5* directly. This result does not concur with the findings of some other studies. For example, using *in situ* hybridization, Richard *et al.* (2003) identified *AQP1*, not *AQP5*, as the estrogen response gene. This discrepancy may have arisen through differences in the methods of detection, since in general, quantitative PCR is more accurate for the evaluation of changes in mRNA than *in situ* hybridization. Actually, recent study using mouse cervix detected the expression of *AQP5* by Northern hybridization (Anderson *et al.* 2006). In addition, Jablonski *et al.* (2003) did not detect expression of *AQP5* at the protein level in the uterus; again, these discrepancies may be a result of differences in experimental design. However, our study clearly detected activation of *AQP5* via both DNA microarray and quantitative PCR, strongly supporting the suggestion that *AQP5* is an estrogen target gene in the uterus. One of the prominent effects of estrogen is water imbibition and for the regulation of water transportation, *AQP5* may play critical role.

Estrogen response and aquaporin

As indicated in Table 2, half ERE could be found in 5′ flanking regions of several AQP genes, but only the ERE motif found in *AQP5* was functional. Our chromatin immunoprecipitation analysis suggested that the half EREs except for *AQP5* were not functional. One possibility is that the EREs were not accessible to ER, but this is less likely because we could detect acetylation of Lys 9 of histon H3 in the region. Although requirement of the *cis* element necessary for ER binding is still not clear, accumulation and analysis of functional EREs *in vivo* such as this study may be important. On the other hand, we could not identify functional ERE of *AQP8* in its 5′ flanking region. As we could not detect genome DNA fragment adjacent to *AQP8*, it is possible that other functional ERE exist in other regions or this gene was activated in secondary effect of estrogen. Recently, we found that adrenomedulin (ADM) gene is a direct target gene of estrogen. *ADM* is activated 1–2 h after estrogen administration and begins to decrease its expression before 6 h. Interestingly, this temporal gene expression profile is very similar to *AQP5*. On the other hand, the temporal gene expression profile of *AQP8* was slightly different and its gene expression level did not change over 12 h. Relevance of direct ER binding and temporal gene expression pattern is one of the intriguing questions.

AQP5 is expressed at high levels in the salivary and lachrymal glands (Raina *et al.* 1995), which are target tissues of Sjogren's syndrome, an autoimmune disorder that occurs primarily in females. A relationship between *AQP5* and this syndrome has been reported (Steinfeld *et al.* 2001; Tsubota *et al.* 2001). In addition, a recent study has suggested that estrogen may affect lymphopoiesis (Shim *et al.* 2004). Therefore, although it remains unclear whether *AQP5* expression in the salivary and lachrymal glands is activated by estrogen, the presence of an ERE motif in the promoter region of this gene suggests the possibility of a functional relationship under certain conditions.

Experimental procedures

Animals

Female C57BL/6 J mice were housed under a 12 h light/dark cycle at 23–25 °C, fed laboratory chow (CE-2; CLEA, Tokyo, Japan) and provided with access to tap water. In order to assess the effect of estrogen on uterine gene expression, 8-week-old mice were ovariectomized and two weeks later injected intraperitoneally with 50 μg/kg body weight of 17β-oestradiol (E2) (Sigma-Aldrich Japan, Tokyo, Japan) or sesame oil (Nacalai Tesque, Kyoto, Japan) as a vehicle control. The whole uterus was collected immediately or at the following times after treatment 1, 2, 6, 12 or 24 h. All animal experiments were approved by the institutional Animal Care Committee.

Chromatin-immunoprecipitation-mediated target cloning

The mouse uterus was fixed with 1% formaldehyde and homogenized in phosphate buffered saline (PBS) containing 0.125 M glycine, using a Physcotron (NS-310E, Microtec, Chiba, Japan). The homogenates were centrifuged at 700 *g* for 5 min at 4 °C and the pellets incubated in lysis buffer (10 mM Tris-HCl [pH 8.0], 10 mM EDTA [pH 8.0], 0.5 mM EGTA and 0.25% Triton X-100) for 10 min. The samples were harvested by microcentrifugation, the pellets resuspended in sonication buffer (10 mM Tris-HCl [pH 8.0], 100 mM NaCl, 1 mM EDTA [pH 8.0], 0.5 mM EGTA), and sonicated using a Bioruptor sonicator (Cosmo Bio, Tokyo, Japan), resulting in DNA with an average length of ~500 bp. Sonicated samples were centrifuged at 15 000 r.p.m. to remove debris and loaded on to a cesium chloride step gradient containing 1.5 mL of 1.75 g/mL CsCl, 1.5 mL of 1.5 g/mL CsCl, and 1 mL of 1.3 g/mL CsCl supplemented with 0.5% (v/v) N-lauroylsarcosine. Samples were centrifuged at 44 000 r.p.m. in a SW55Ti rotor for 24 h. 0.1 mL fractions were collected from the bottom of the gradient and fractions containing cross-linked chromatin were

© 2006 The Authors
Journal compilation © 2006 by the Molecular Biology Society of Japan/Blackwell Publishing Ltd.

combined and dialyzed vs. TE buffer. Then the samples were precleared with protein G Sepharose for 1 h at 4 °C and incubated with either 10 μg anti-ERα polyclonal rabbit antibody (H-184; Santa Cruz, CA, USA) overnight at 4 °C. The sample was precipitated with protein G Sepharose, washed 5 times with RIPA buffer (10 mM Tris-HCl [pH 8.0], 140 mM NaCl, 1 mM EDTA [pH 8.0], 0.5 mM EGTA, 1% Triton X-100, 0.1% SDS, 0.1% sodium deoxycholate), then recovered by incubation in elution buffer (0.1 M sodium bicarbonate, 1% SDS). Cross-linking was reversed by incubation for 6 h at 65 °C, followed by incubation with proteinase K for 4 h at 45 °C. Samples were extracted with phenol/chloroform and ethanol precipitated. The precipitated DNA fragments were cloned into pGEM-T vactor (Promega, Tokyo, Japan) by ligation-mediated PCR (LMPCR). Briefly, the DNA fragment was blunt ended and phosphorylated with T4 DNA polymerase (Takara Bio Inc., Shiga, Japan) and T4 polynucleotide kinase (Takara Bio Inc., Shiga, Japan), respectively. After ligating oligonucleotide linkers, the DNA fragment was amplified by PCR and cloned. Oligonucleotide sequences of the linker were F 5′-GCGGTGACCCGGGAGATCTGAATTC-3′ and R 5′-GAATTCAGATC-3′. PCR amplification was performed in the presence of 0.1 nM primer "F," 0.2 mM of each nucleotide (dATP, dCTP, dGTP and dTTP), 1 × PCR buffer and 1 U of LA Taq (Takara Bio Inc., Shiga, Japan) in 20 μL of reaction buffer. After 30 amplification cycles, the PCR products were purified with QIAquick PCR purification kit (QIAGEN, Tokyo, Japan) and cloned into pGEM-T easy vector. Colonies were randomly picked up after transformation and inserted sequences were analyzed.

Chromatin immunoprecipitation

Mouse uterine genomic DNA was prepared and sonicated as described above. The sonicated samples were precleared with protein G Sepharose for 1 h at 4 °C, then incubated with either 10 μg anti-ERα polyclonal rabbit antibody (Santa Cruz, CA, USA) or 10 μg anti-acetylated histone H3 (Lys9) antibody (Cell Signaling, Danvers, MA, USA) overnight at 4 °C. The samples were precipitated with protein G Sepharose, washed 5 times with RIPA buffer (10 mM Tris-HCl [pH 8.0], 140 mM NaCl, 1 mM EDTA [pH 8.0], 0.5 mM EGTA, 1% Triton X-100, 0.1% SDS, 0.1% sodium deoxycholate), then recovered by incubation in elution buffer (0.1 M sodium bicarbonate, 1% SDS). Cross-linking was reversed by incubation for 6 h at 65 °C, followed by incubation with proteinase K for 4 h at 45 °C. Samples were extracted with phenol/chloroform and ethanol precipitated. In general, 1/30th of the precipitated DNA was used in a PCR amplification reaction. PCR amplification was performed in the presence of 0.1 nM primers, 0.2 mM of each nucleotide (dATP, dCTP, dGTP and dTTP), 1 × PCR buffer and 1 U of AmpliTaq Gold (PerkinElmer Japan, Tokyo, Japan) in 20 μL of reaction buffer. After 35 amplification cycles, the PCR products were analyzed using agarose electrophoresis. As a negative control, the same experiments were performed with IgG. Primer sequences used to amplify the precipitated DNA are listed in Tables 1 and 2.

Preparation of labeled cRNA and microarray analysis

Total uterine RNA was extracted using TRIzol reagent (Invitrogen, Tokyo, Japan) and the RNeasy total RNA purification kit (Qiagen, Tokyo, Japan). cRNA probes were prepared from purified RNA using a CodeLink Expression assay reagent kit (Amersham Bioscience K.K., Tokyo, Japan). The amplified cRNA (10 μg) was hybridized to oligonucleotide DNA microarrays (CodeLink Uniset Mouse I Bioarray, Amersham Bioscience K.K., Tokyo, Japan), which were scanned and processed using a GenePix 4000B scanner and GenePix Pro software (Axon Instruments, Union City, CA, USA), respectively. In order to confirm the estrogen-related changes in gene expression revealed by DNA microarray analysis, the experiment was repeated independently at least twice. The expression data were analyzed using GeneSpring software (Agilent Tech. Japan, Tokyo, Japan).

Quantitative real time-PCR

cDNA was synthesized from total RNA purified using Superscript II RT(-) (Invitrogen) and random primers at 42 °C for 60 min. Quantitative PCR reactions were performed according to the manufacturer's instructions, using the PE Prism 7000 sequence detector (Applied Biosystems, Tokyo, Japan), SYBR-Green PCR Core Reagents (Applied Biosystems) and primers designed for amplification of short PCR products (< 100 bp; Table 3).

Plasmid construction

A DNA fragment encoding mouse ERα was amplified from uterine cDNA using the primers 5′-GGCGAATTCATGACCATGACCCTTCACAC-3′ and 5′-GCAGTCGACTCAGATCGTGTTGGGGAAGC-3′, digested with *Eco*RI and *Sal*I, then ligated into pcDNA3.1(+) (Invitrogen), generating pERαcDNA3.1.

The 5′ flanking regions of AQP genes were amplified using the primers listed in Table 3, then digested with *Mlu*I and *Bgl*II and ligated into pGL2-basic (Promega, Tokyo, Japan). Inserts for the shorter *AQP5* reporters, p103AQP5-luc and p13AQP5-luc (5′ regions flanking *AQP5*, -103 to +74 and -13 to +74, respectively), were amplified using the forward primers 5′-cgacgcgtTGGGTGAGACCGACCGGGTCAAGATG-3′ and 5′-cgacgcgtAAAGGCCGGCCGGAGAGGGA-3′, respectively. The primer 5′-cgacgcgtTGGGTGAGACCGACCGaaTCAAGATGCTCC-3′ was used for amplification of the mutated ERE reporter (pm103AQP5-luc).

Luciferase reporter assay

HEK293T cells were cultured in Dulbecco's Modified Eagle's Medium (DMEM) supplemented with 10% fetal bovine serum. For ligand-dependent transcription assays, cells were seeded in 24-well tissue culture plates and grown in phenol red-free DMEM supplemented with 5% charcoal/dextran-treated fetal calf serum (JRH Biosciences, Inc. Lenexa, KS, USA). HEK293T cells were

© 2006 The Authors
Journal compilation © 2006 by the Molecular Biology Society of Japan/Blackwell Publishing Ltd.

© 2006 The Authors
Journal compilation © 2006 by the Molecular Biology Society of Japan/Blackwell Publishing Ltd.

Table 3 Primer sequences for quantitative PCR and cloning

Gene	RefSeq number	Q-PCR Direction	Position	Sequence	Reporter position	Sequence
AQP1	NM_007472	F	2246	TCACAGCTGCACACTCGTCTC	−932	cgacgcgtCCACTTTCCACCATCACTCG
		R	2319	TGGGTCCTCAGTGCCCTTAT	28	gaagatctCTCGACTTAACCGCTGGATG
AQP2	NM_009699	F	1237	GGGTGTAAAAGTGCTCGTCCAT	−917	cgacgcgtCTGTGGTAAGGGTGGCTCTG
		R	1287	TCTGCACGTGAGGAAAGAAACA	30	gaagatctGCTCTTCCTCCCTCCCTCTC
AQP3	NM_016689	F	1535	GGCTGAAGTCCAGGTCGTAAGT	−868	cgacgcgtGCACTGCTATGAACGTGTGG
		R	1634	GGAGTTTCCCACCCCTATTCC	66	gaagatctCAACTCCTTCTGTCGACCCA
AQP4	NM_009700	F	1030	GAGGACAGCACTGAAGGCAGA	−939	cgacgcgtTTAAGAGCCAGAGAACCTAC
		R	1097	TCCTTAATGGGTGGCAGGAA	74	gaagatctGTGCTGAGCATTGTTTCCTG
AQP5	NM_009701	F	1527	TTGTGAAGGCAGTGCAAGCT	−611	cgacgcgtCGCAGAAACGCAGGAACACA
		R	1579	CACCCCTTTCTGGGATGGT	74	gaagatctGTGCGTGCTGGGCTCTCCTG
AQP6	NM_175087	F	1436	TGGATCCCTGTCTTGGAGAAA	−998	cgacgcgtAGACAGGGAGGGTGGCATTT
		R	1517	TGGGCTCTGAAGCTCCTTCAT	70	gaagatctGCCAGGAACTCAGCAAAAAG
AQP7	NM_007473	F	2206	TCAAGACAGGGTTTCTCGGTG	−988	cgacgcgtCATGGGTGCAGGCTACAGAC
		R	2294	AGGCAGGCGGATTTCTGAG	63	gaagatctTGTCTTTCAGCCTCCGTCTC
AQP8	NM_007474	F	1220	GGGATTAGAAGGGCTGAGAAGG	−943	cgacgcgtTCAGACAAGAAGCGGCAGAG
		R	1311	GAATTGGGTTCCAAACCCAAC	47	gaagatctTCTAGGTCACAGACTGGAGG
AQP9	NM_022026	F	2061	TGACCTGAGCAAGTTGCCCT	NT	
		R	2140	CAGTCGGCTAGCAAGCTTCTG		
AQP11	NM_175105	F	1110	CAGTCAAGCTGGATGCGACA	NT	
		R	1172	AAGCTGAAGCAGGAGGCGT		
AQP12	NM_177587	F	924	CCGGCAGAAAAGCAAATACC	−981	cgacgcgtTTTGCTTAGCCTGTCCTGTG
		R	1019	ACGGCCCTTTGCCACTACT	54	gaagatctTGGGTTCTACAAGGAGCAAG

transfected using FuGene6 (Roche Diagnostics K.K., Tokyo, Japan), following the manufacturer's instructions, and the following day treated with either ethanol or 10 nM E2. Typically, cells were transfected with 0.3 μg luciferase reporter plasmid, 50 ng pERαcDNA3.1 (ERα expression plasmid) or 50 ng pRL-TK reporter plasmid (cDNA encoding *Renilla* luciferase downstream of the thymidine kinase promoter) (Promega, Tokyo, Japan). Luciferase values were normalized to the *Renilla* luciferase activity.

Acknowledgements

This work was supported in part by a Core Research for Evolutional Science research grant from the Japan Science and Technology Cooperation, a Grant-in-Aid for Scientific Research from the Japan Society for the Promotion of Science, a Grant-in-Aid for Scientific Research from the Ministry of Education, Culture, Sports, Science and Technology of Japan, a Health Sciences Research Grant from the Ministry of Health, Labour and Welfare of Japan, a research grant from the Ministry of Environment, Japan.

References

Anderson, J., Brown, N., Mahendroo, M.S. & Reese, J. (2006) Utilization of different aquaporin water channels in the mouse cervix during pregnancy and parturition and in models of preterm and delayed cervical ripening. *Endocrinology* **147**, 130–140.

Bourdeau, V., Deschenes, J., Metivier, R., Nagai, Y., Nguyen, D., Bretschneider, N., Gannon, F., White, J.H. & Mader, S. (2004) Genome-wide identification of high-affinity estrogen response elements in human and mouse. *Mol. Endocrinol.* **18**, 1411–1427.

Carroll, J.S., Liu, X.S., Brodsky, A.S., Li, W., Meyer, C.A., Szary, A.J., Eeckhoute, J., Shao, W., Hestermann, E.V., Geistlinger, T.R., Fox, E.A., Silver, P.A. & Brown, M. (2005) Chromosome-wide mapping of estrogen receptor binding reveals long-range regulation requiring the forkhead protein FoxA1. *Cell* **122**, 33–43.

Cullinan-Bove, K. & Koos, R.D. (1993) Vascular endothelial growth factor/vascular permeability factor expression in the rat uterus: rapid stimulation by estrogen correlates with estrogen-induced increases in uterine capillary permeability and growth. *Endocrinology* **133**, 829–837.

Heinemeyer, T., Chen, X., Karas, H., Kel, A.E., Kel, O.V., Liebich, I., Meinhardt, T., Reuter, I., Schacherer, F. & Wingender, E. (1999) Expanding the TRANSFAC database towards an expert system of regulatory molecular mechanisms. *Nucleic Acids Res.* **27**, 318–322.

Hertz, G.Z. & Stormo, G.D. (1999) Identifying DNA and protein patterns with statistically significant alignments of multiple sequences. *Bioinformatics* **15**, 563–577.

Hewitt, S.C., Deroo, B.J., Hansen, K., Collins, J., Grissom, S., Afshari, C.A. & Korach, K.S. (2003) Estrogen receptor-dependent genomic responses in the uterus mirror the biphasic physiological response to estrogen. *Mol. Endocrinol.* **17**, 2070–2083.

Inoue, S., Orimo, A., Hosoi, T., Kondo, S., Toyoshima, H., Kondo, T., Ikegami, A., Ouchi, Y., Orimo, H. & Muramatsu, M. (1993) Genomic binding-site cloning reveals an estrogen-responsive gene that encodes a RING finger protein. *Proc. Natl. Acad. Sci. USA* **90**, 11117–11121.

Jablonski, E.M., McConnell, N.A., Hughes, F.M. Jr & Huet-Hudson, Y.M. (2003) Estrogen regulation of aquaporins in the mouse uterus: potential roles in uterine water movement. *Biol. Reprod.* **69**, 1481–1487.

Kahlert, S., Nuedling, S., van Eickels, M., Vetter, H., Meyer, R. & Grohe, C. (2000) Estrogen receptor α rapidly activates the IGF-1 receptor pathway. *J. Biol. Chem.* **275**, 18447–18453.

Kamalakaran, S., Radhakrishnan, S.K. & Beck, W.T. (2005) Identification of estrogen-responsive genes using a genome-wide analysis of promoter elements for transcription factor binding sites. *J. Biol. Chem.* **280**, 21491–21497.

Krege, J.H., Hodgin, J.B., Couse, J.F., Enmark, E., Warner, M., Mahler, J.F., Sar, M., Korach, K.S., Gustafsson, J.A. & Smithies, O. (1998) Generation and reproductive phenotypes of mice lacking estrogen receptor beta. *Proc. Natl. Acad. Sci. USA* **95**, 15677–15682.

Laganiere, J., Deblois, G., Lefebvre, C., Bataille, A.R., Robert, F. & Giguere, V. (2005) From the Cover: Location analysis of estrogen receptor alpha target promoters reveals that FOXA1 defines a domain of the estrogen response. *Proc. Natl. Acad. Sci. USA* **102**, 11651–11656.

Li, X., Yu, H. & Koide, S.S. (1994) The water channel gene in human uterus. *Biochem. Mol. Biol. Int.* **32**, 371–377.

Lindsay, L.A. & Murphy, C.R. (2004) Redistribution of aquaporins in uterine epithelial cells at the time of implantation in the rat. *Acta Histochem.* **106**, 299–307.

Lubahn, D.B., Moyer, J.S., Golding, T.S., Couse, J.F., Korach, K.S. & Smithies, O. (1993) Alteration of reproductive function but not prenatal sexual development after insertional disruption of the mouse estrogen receptor gene. *Proc. Natl. Acad. Sci. USA* **90**, 11162–11166.

Migliaccio, A., Di Domenico, M., Castoria, G., de Falco, A., Bontempo, P., Nola, E. & Auricchio, F. (1996) Tyrosine kinase/p21ras/MAP-kinase pathway activation by estradiol-receptor complex in MCF-7 cells. *EMBO J.* **15**, 1292–1300.

Moggs, J.G., Tinwell, H., Spurway, T., Chang, H.S., Pate, I., Lim, F.L., Moore, D.J., Soames, A., Stuckey, R., Currie, R., Zhu, T., Kimber, I., Ashby, J. & Orphanides, G. (2004) Phenotypic anchoring of gene expression changes during estrogen-induced uterine growth. *Environ. Health Perspect.* **112**, 1589–1606.

O'Lone, R., Frith, M.C., Karlsson, E.K. & Hansen, U. (2004) Genomic targets of nuclear estrogen receptors. *Mol. Endocrinol.* **18**, 1859–1875.

Offenberg, H., Barcroft, L.C., Caveney, A., Viuff, D., Thomsen, P.D. & Watson, A.J. (2000) mRNAs encoding aquaporins are present during murine preimplantation development. *Mol. Reprod. Dev.* **57**, 323–330.

Raina, S., Preston, G.M., Guggino, W.B. & Agre, P. (1995) Molecular cloning and characterization of an aquaporin cDNA from salivary, lacrimal, and respiratory tissues. *J. Biol. Chem.* **270**, 1908–1912.

Richard, C., Gao, J., Brown, N. & Reese, J. (2003) Aquaporin water channel genes are differentially expressed and regulated

© 2006 The Authors
Journal compilation © 2006 by the Molecular Biology Society of Japan/Blackwell Publishing Ltd.

by ovarian steroids during the periimplantation period in the mouse. *Endocrinology* **144**, 1533–1541.

Richards, E.J. & Elgin, S.C. (2002) Epigenetic codes for heterochromatin formation and silencing: rounding up the usual suspects. *Cell* **108**, 489–500.

Shim, G.J., Warner, M., Kim, H.J., Andersson, S., Liu, L., Ekman, J., Imamov, O., Jones, M.E., Simpson, E.R. & Gustafsson, J.A. (2004) Aromatase-deficient mice spontaneously develop a lymphoproliferative autoimmune disease resembling Sjogren's syndrome. *Proc. Natl. Acad. Sci. USA* **101**, 12628–12633.

Simoncini, T., Hafezi-Moghadam, A., Brazil, D.P., Ley, K., Chin, W.W. & Liao, J.K. (2000) Interaction of oestrogen receptor with the regulatory subunit of phosphatidylinositol-3-OH kinase. *Nature* **407**, 538–541.

Steinfeld, S., Cogan, E., King, L.S., Agre, P., Kiss, R. & Delporte, C. (2001) Abnormal distribution of aquaporin-5 water channel protein in salivary glands from Sjogren's syndrome patients. *Lab. Invest.* **81**, 143–148.

Tsubota, K., Hirai, S., King, L.S., Agre, P. & Ishida, N. (2001) Defective cellular trafficking of lacrimal gland aquaporin-5 in Sjogren's syndrome. *Lancet* **357**, 688–689.

Watanabe, H., Suzuki, A., Goto, M., Lubahn, D.B., Handa, H. & Iguchi, T. (2004) Tissue-specific estrogenic and non-estrogenic effects of a xenoestrogen, nonylphenol. *J. Mol. Endocrinol.* **33**, 243–252.

Watanabe, H., Suzuki, A., Kobayashi, M., Takahashi, E., Itamoto, M., Lubahn, D.B., Handa, H. & Iguchi, T. (2003) Analysis of temporal changes in the expression of estrogen-regulated genes in the uterus. *J. Mol. Endocrinol.* **30**, 347–358.

Watanabe, H., Suzuki, A., Mizutani, T., Khono, S., Lubahn, D.B., Handa, H. & Iguchi, T. (2002) Genome-wide analysis of changes in early gene expression induced by oestrogen. *Genes Cells* **7**, 497–507.

Wei, C.L., Wu, Q., Vega, V.B., *et al.* (2006) A global map of p53 transcription-factor binding sites in the human genome. *Cell* **124**, 207–219.

Wong, C.W., McNally, C., Nickbarg, E., Komm, B.S. & Cheskis, B.J. (2002) Estrogen receptor-interacting protein that modulates its nongenomic activity-crosstalk with Src/Erk phosphorylation cascade. *Proc. Natl. Acad. Sci. USA* **99**, 14783–14788.

Received: 10 April 2006
Accepted: 17 May 2006

© 2006 The Authors
Journal compilation © 2006 by the Molecular Biology Society of Japan/Blackwell Publishing Ltd.

Available online at www.sciencedirect.com
SCIENCE DIRECT
Reproductive Toxicology 22 (2006) 20–29
Reproductive Toxicology
www.elsevier.com/locate/reprotox

Effects of bisphenol A given neonatally on reproductive functions of male rats

Hideo Kato [a,b,c], Tadakazu Furuhashi [a], Masami Tanaka [d], Yoshinao Katsu [c], Hajime Watanabe [c], Yasuhiko Ohta [e], Taisen Iguchi [c,*]

[a] *Nihon Bioresearch Inc., 6-104 Majima, Fukuju-cho, Hashima 501-6251, Japan*
[b] *The United Graduate School of Veterinary Science, Yamaguchi University, 1677-1, Yoshida 753-8515, Japan*
[c] *Okazaki Institute for Integrative Bioscience, National Institute for Basic Biology, National Institutes of Natural Sciences, 5-1, Higashiyama, Myodaiji, Okazaki, Aichi 444-8787, Japan*
[d] *Department of Pharmacology, St. Marianna University School of Medicine, 2-16-1, Sugao, Miyamae, Kawasaki 216-8511, Japan*
[e] *Laboratory of Experimental Animal Science, Department of Veterinary Medicine, Faculty of Agriculture, Tottori University, 4-101 Minami, Koyama, Tottori 680-8553, Japan*

Received 9 April 2005; received in revised form 5 September 2005; accepted 21 October 2005
Available online 28 November 2005

Abstract

Male Sprague–Dawley rats (Crj:CD (IGS) were treated neonatally with bisphenol A (BPA) to evaluate effects on reproductive parameters. Animals were given BPA subcutaneously in corn oil to dosages of 0.002–97 mg/kg body weight, or 0.9 mg/kg 17β-estradiol (E2) once a day from postnatal day (PND) 0 to PND 9. Preputial separation, copulatory rate, fertility rate, sperm analysis, serum testosterone levels, and gene expression in the testis were assessed. Males in the E2 group showed a decrease in testis weight and alterations of estrogen-mediated gene expression in the testis on PND 10, and by PND 150 incomplete preputial separation, decreases in the copulatory rate, testicular and accessory organ weights and number of sperm. In contrast, males in all BPA groups showed normal reproductive parameters. These results indicate that in male rats, BPA given during the neonatal period neither affected reproductive function nor evoked estrogen-mediated gene responses in the testis.
© 2005 Elsevier Inc. All rights reserved.

Keywords: Bisphenol A; Low dose; Reproductive function; Neonatal period; Male rat; Gene expression; 17β-estradiol

1. Introduction

The relationship between chemical pollution and reproductive health is of major public health concern. Some etiological studies have disclosed regional declines in sperm count [1,2] and increases in hypospadias [3]; however, some studies have not reported similar findings [4–9]. The relation between chemical pollution and reproductive abnormalities has also been described in wildlife [10]. Such abnormalities have been attributed partly to estrogenic activity of the contaminants [3]. A potent synthetic estrogen, diethylstilestrol (DES) administered as a pharmaceutical agent to pregnant women between the late 1940s and early 1970s in the USA and Europe resulted in an increase in the risk of urogenital tract abnormalities, the so-called DES syndrome, in daughters and sons of DES treated women [11–13].

Bisphenol A (BPA) is used in the manufacture of polystyrene and epoxy resins. It is reported to have weak binding affinity to the estrogen receptors (ER)α and ERβ [14] and scant estrogenic activity when measured by the yeast two-hybrid assay [15]. Nevertheless, BPA has been detected in human urine [16], maternal blood samples [17], fetal placental units [17–20], and ovarian follicular fluids [20].

Oral administration of BPA at very low-dose levels (2 and 20 μg/kg) has been reported to cause reduced sperm production [21] and increased prostate weight [22]. These effects were reported in CF-1 mice exposed orally during prenatal development from gestation day (GD) 11 to GD 17, but comparable to the dose to which humans are usually exposed to in their daily lives. Results with BPA at low-dose levels given to mothers have been inconsistent. Some studies reported reproductive changes in male offspring including a reduction of sperm production

* Corresponding author. Tel.: +81 564 59 5235; fax: +81 564 59 5236.
E-mail address: taisen@nibb.ac.jp (T. Iguchi).

0890-6238/$ – see front matter © 2005 Elsevier Inc. All rights reserved.
doi:10.1016/j.reprotox.2005.10.003

[23–25], whereas others failed to demonstrate these changes [26–28]. The National Toxicology Program has evaluated the discrepancies in the scientific evidence on low-dose effects [29]. The preponderance of evidence favored the conclusion that there are no low-dose effects of BPA; however, the possibility of a low-dose effect could not be discounted because the effects being measured were subtle and can be influenced by large number of variables that are difficult to control.

Most studies were conducted to expose mothers, but not neonates, to low-dose levels of BPA. In male rats and mice, neonatal treatment of estrogen for 10–30 days results in a long-lasting suppression of spermatogenesis [30,31]; however, if the commencement of estrogen injection is delayed until the 10th postnatal day, then a permanent arrest of spermatogenesis takes place in rats and mice [32,33].

The present study has evaluated the effect of neonatal exposure of low dose of BPA in male rats. BPA treatment was by subcutaneous administration as the dosing route rather than oral administration to replicate exposure conditions of a former experiment that studied BPA in neonatal female rats [34]. Low-dose effects on male reproductive functions were analyzed using end points for general reproductive toxicity studies. Under the hypothesis that male reproductive parameters would be adversely affected by BPA exposure, we analyzed gene expression for the steroidogenic enzymes in the testis. Quantification of gene expression, which was identified by the subpanel of the National Toxicology Program as an additional research to clarify uncertainties [29], is sensitive and easily measured molecular end point.

2. Materials and methods

2.1. Animal rearing and treatment

Pregnant Sprague–Dawley rats (Crj:CD, IGS) were used in this study. The animals were housed individually in cages placed in an animal room on a 12-h light/12-h dark cycle (lighting: 06:00–18:00 h) with controlled temperature (21–25 °C), relative humidity (45–65%), and filter-sterilized fresh air changes. The animals were given free access to CRF-1 diet manufactured from natural raw materials (Oriental Yeast Co., Ltd., Tokyo, Japan) and tap water ad libitum. Estrogenic activity of CRF-1 diet is relatively low compared to the other commercially available certified rodent diets in Japan [35]. Twelve dams which spontaneously delivered offspring on the same day were used for each of three tests, in which the neonates were necropsied on PND 10, PND 35, or PND 150. The day of delivery was defined as PND 0. A total of 56 male neonates whose body weights were similar were selected from all male neonates delivered, and eight foster mothers nursed seven male neonates each. Seven males from each litter were allotted to seven groups. The remaining males and all female neonates were not used in this study. The male neonates were given the vehicle (ethanol) only, which served as the control, 24 ng, 120 ng, 600 ng, 3 μg, or 1 mg of bisphenol A [BPA; 2,2-bis (4-hydroxyphenol) propane, Kanto Chemical Co., Inc., Tokyo, Japan], or 10 μg of 17β-estradiol (E2, Sigma Chemical Co., St. Louis, MO) once a day from PNDs 0 to 9. BPA was dissolved in ethanol (Wako Pure Chemical Industries, Ltd., Osaka, Japan) to 500 mg/ml. The solution thus prepared was diluted with ethanol to BPA concentrations of 12, 60, 300, and 1500 μg/ml. Each dilution prepared was mixed with corn oil (Wako) to a concentration of 1/10. The control group was treated with a mixture of ethanol and alcohol at a volumetric ratio of 1:9. E2 was likewise dissolved at a dose of 500 μg/ml in the ethanol–oil solution. The animals were given a subcutaneous injection of 0.02 ml solution dorsally. To test effects of BPA on three different progressive stages, necropsy was performed on PNDs 10, 35, and 150. At all stages, eight male neonates of each group were given the vehicle, BPA, or E2.

Average doses of BPA in the present study were calculated on the basis of the body weight from PNDs 0 to 9 as reported previously [34]: the doses of BPA per kg body weight were 2 μg (1–3.5 μg) in the 24 ng group, 11 μg (4.8–18 μg) in the 120 ng group, 56 μg (24–87 μg) in the 600 ng group, 277 μg (124–429 μg) in the 3 μg group and 97 mg (43–152 mg/kg) in the 1 mg group. The dose of E2 per kg body weight was 0.9 mg (0.4–1.4 mg) in the 10 μg group.

For animals necropsied on PND 10, the serum testosterone levels and the testicular weight were measured, and histological changes and gene expression in the testis were examined. For animals necropsied on PND 35, in addition to the parameters on PND 10, the seminal vesicle, ventral prostate, and epididymis were weighed. For animals necropsied on PND 150, the males were weaned on PND 21, checked for preputial separation daily from PNDs 35 to 70, and bred to untreated females from PNDs 105 to 130 for confirmation of the fertility. On PND 150, all males were sacrificed to measure some sperm parameters in the left cauda epididymis, gene expression in the testis and serum testosterone levels, and to examine histology of the testis and ventral prostate. At the same time, the organs corresponding to those which were weighed on PND 35 were weighed.

The right testis on PNDs 10, 35, and 150, and ventral prostate on PND 150 were fixed in 10% neutral buffered formalin, cut in paraffin at 4 μm, and stained routinely with hematoxylin and eosin for histological examination. The left testis on PNDs 10, 35, and 150, and left cauda epididymis on PND 150 were frozen in liquid nitrogen and stored at −80 °C until use.

2.2. Mating and cesarean section

The males were paired and mated with untreated females at proestrus on a one-to-one basis from the evening (about 17:00 h) to the next morning (about 09:00 h). Females which had sperm in the vaginal smear the next morning were regarded as having copulated. The day when the sperm was found was defined as Day 0 of gestation. Males which failed to copulate were separated once from the females and mated again with other untreated females at proestrus 3 or 4 days later. Thus, the males were mated with untreated females a maximum of four times until evidence of copulation was observed. Females in which copulation had been confirmed were subjected to Caesarean section on Day 13 of gestation and examined for the number of corpora lutea, embryonic mortality, and implantation sites.

2.3. Measurements of serum testosterone levels

The serum testosterone level was estimated by commercially available radioimmunoassay kit (rat testosterone RIA kit, IMMUNOTECH, Marseille, France). Regarding the serum samples obtained on PND 10, the serum from two to three animals in the same group were stored at −20 °C until use. Testosterone was extracted from the serum with diethyl ether in a volume 10 times as much as the volume of the serum in order to concentrate testosterone because the serum testosterone level on PND 10 was under the lower limit of quantitative analysis (5 ng/ml). The organic and aqueous phases were separated by the dry ice–ethanol method. The ether phase was evaporated by ventilation and reconstituted in a serum diluent provided with the RIA kit. In contrast, the serum samples obtained on PNDs 35 and 150 were subjected to the measurement for each animal without extraction.

2.4. Sperm analysis

To prepare semen samples, the right cauda epididymis was cut into strips in culture fluid for sperm (Medium 199 with 0.5% BSA) at 37 °C and left still for about 5 min. The prepared semen samples were examined for: (1) sperm motility and (2) sperm morphology as described below. Suspensions of sperm were prepared using the left cauda epididymis to examine (3) the number of sperm.

2.4.1. Sperm motility

The diluted semen sample was put into a sample chamber (MICROSLIDES, #HTR1099, VitroCom INC., NJ, USA) to calculate the motile sperm rate (%) and progressive sperm rate (%) using TOX IVOS (Hamilton Thorne Research,

MA, USA). Measurement of sperm motility was performed after the diluted semen sample which was incubated in a CO_2 incubator for 30 min.

2.4.2. Sperm morphology

The semen sample was smeared on a glass slide, fixed in 10% neutral buffered formalin, and stained with 1% eosin solution. Morphology of 300 sperm was observed under a microscope.

2.4.3. Number of sperm

The left cauda epididymis was homogenized (Ultra-Turrax T25 basic, IKA-Labortechnic, Germany) and put into a sample chamber (2X-CEL, Fertility Technologies, Inc., NY, USA). Then the number of sperm was counted using TOX IVOS. The number of sperm per gram was obtained by dividing the number of sperm by weight of the cauda epididymis.

2.5. RNA isolation and quantitative RT-PCR

Total RNA from the testis was isolated using ISOGEN (NIPPON GENE, Tokyo, Japan), purified using an RNeasy kit (QIAGEN, Chatsworth, CA, USA) according to the manufacturer's protocol, and then stored at −80 °C until use. For RT-PCR, each RNA was treated with ribonuclease free deoxyribonuclease 1 (Invitrogen, Co., CA, USA). Then, 1 μg of total RNA was reverse transcribed using random primer and superscript 11 reverse transcriptase (Invitrogen) at 42 °C for 60 min. PCR was carried out in the ABI Prism 5700 Sequence Detection System (Applied Biosystems, CA, USA) using SYBER Green Master Mix (Applied Biosystems) in the presence of appropriate gene primers. Sequences of gene primer sets are given in Table 1. We examined the expression of ERα, ERβ, progesterone receptor (PR), androgen receptor (AR), cholesterol side-chain cleavage enzyme (P450scc), 17α-hydroxylase-17, 20-lyase (CYP17), 3β-hydroxysterod dehydrogenase (3β-HSD), 17β-hydroxysterod dehydrogenase (17β-HSD), and cytocrome P450 subfamily 19 (CYP19). Relative RNA equivalents for each sample were obtained by standardization of glyceraldehyde-3-phosphate dehydrogenase (GAPDH). Each PCR amplification was performed in triplicate, under the following conditions: 2 min at 50 °C and 10 min at 95 °C, followed by a total of 40 two-temperature cycles (15 s at 95 °C and 1 min at 60 °C in a volume of 15 μl).

2.6. Statistics

Data were statistically analyzed by multiple comparison tests as described below and compared for body weight, organ weight, parameters for observation of fetuses and preputial separation and for sperm analysis, and serum testosterone level between the control group and each of the groups treated with BPA. Group mean values and standard errors were calculated. Subsequently, the data on the BPA groups were tested by Bartlett's method for homogeneity of variance. When the variances were homogenous, Dunnett's method was used. When the variances were heterogeneous, a Dunnett-type method using a rank order was used. Data on the E2 group were tested by Student's *t*-test and compared with the control group. The copulatory rate and fertility rate obtained in the BPA groups and E2 group were tested by Fisher's exact probability test. The level of significance was set at 5%.

3. Results

3.1. General signs and body weight changes

The injection sites became white in all animals in the 1 mg BPA group a few days after the 1st injection. No such change was noted in any other groups. No animals died in any group until the day of necropsy. There were no significant differences in the body weight among the control, BPA, or E2 group (Table 2).

3.2. Preputial separation

Preputial separation was completed in all males in the BPA groups (Table 3). There were no differences in the day of completion for preputial separation between any of the BPA groups and the control group. On the other hand, preputial separation was incomplete in five of the eight males in the E2 group until PND 150. Preputial separation was noted 2 weeks later in the E2 group than in the control.

3.3. Copulatory rate, fertility rate, and observation of fetuses

Copulation was observed by the second paring in the BPA groups (Table 4). The copulatory rate was 100% in the BPA groups. The fertility rate was 100% in the BPA groups except for the 1 mg group showing 87.5%; the lower fertility rate in the 1 mg group was caused by one female in which no implantation scars were noted. However, one male which failed to fertilize this female was confirmed to have the capability to fertilize later when he was mated with another female. Accordingly, this male was judged to have normal fertilizability. Compared with the control, the copulatory rate was significantly lower in the E2 group. Only three of the eight pairs succeed in copulation; the preputial separation was completed in these pairs. Although they copulated with normal females, one of them failed to fertilize his partner. The male was paired and mated again with another female, but they failed to copulate. Therefore, it was not possible to confirm his fertilizability in the present study.

Table 1
Sequences of gene primer sets for Q-RT-PCR

Gene	GenBank Accession no.	Primer sequences (5′–3′)	
		Forwad	Reverse
ERα	NM_012689	CACACACGCTCTGCCTTGA	GACGGAAGGAAGGAATGTGC
ERβ	U57439	TGGAGATGCTGAATGCTCACAC	TGGCCATCACTGAGACTGTAGG
PR	NM_022847	TGAGAAAGTGCTGTCAGGCTG	TTAGGAAAGGCCACTGACTGG
AR	M23264	TACCCTCCCATGGCACATTT	AAACACAGGCAGGAGCACAAC
P450scc	J05156	CTGTGATTACCTGTCCACGTTAGC	GAAAGGGAGACAGGARGAAAGAGA
P450c17	M31681	ATCCATACCTCAACACCCACAGTA	GCACTGGGACTAGCACCTCTAAGA
3β-HSD	M38179	CAAGCAGAAAACCTCGGAGTG	GGAGGATCCAGTAAACACCCAG
17β-HSD	AF035156	TGGAGGGAGAGTTGAGGAGATC	CCGACGACTACCACCAAGGA
CYP19	M33986	CTGTCCATTCCAGCACCCTTAC	GCACGCAAAGCAGTAGTTTGG
GAPDH	BC059110	AGAGAGAGGCCCTCAGTTGCT	GTGAGGGAGATGCTCAGTGTTG